

UAM Hybrid Power System

Final Report – Team 9

MECH 460: Team Project, Conceive and Design

Department of Mechanical and Materials Engineering

Queen's University

Following the professional engineering practice, we bear the burden of proof for original work. We have read the Policy on Academic Integrity posted on the Faculty of Engineering and Applied Science web site engineering.queensu.ca/policy/Honesty and confirm that this work is in accordance with the policy.

 Date: December 6, 2021

Luke Ulsifer

 Date: December 6, 2021


Charlie Heinzl

 Date: December 6, 2021

Vincent Halis

 Date: December 6, 2021

Alex Parks

 Date: December 6, 2021

Ben Langlois

Based on the information provided to me by the Team, they have satisfactorily completed both the technical work and the deliverables for their project.

 Date: Dec 6, 2021

Professor Kim

Executive Summary

Urban populations are quickly outgrowing existing intracity transportation infrastructure. To meet intracity travel demands, new technology must be developed to alleviate congested ground transportation. Urban Air Mobility (UAM) vehicles are increasingly becoming popular in the aviation industry, due to their small form factor and suitability for short intracity flights and utilization of the relatively empty airspace above cities. UAM vehicles take advantage of vertical takeoff and landing (VTOL) strategy. The Structural and Multidisciplinary System Design (SMSD) team at Queen's University has been working on a UAM vehicle and has requested the design of a hybrid power system. The vehicle must have VTOL capabilities and the ability to complete a 150 km trip while travelling at least 110 km/h, with a desired power system weight of 700 kg or less. The hybrid power system to be developed for the UAM vehicle will consist of a gas turbogenerator, batteries, AC electric motors, and propellers.

To determine an accurate estimate of the power requirements needed for a 150 km trip, a mission simulation was created in Python. The mission simulation is based upon first principles, utilizing free body diagrams and power equations to determine the power output required during the entire trip. This simulation segmented the flight into 3 main sections: vertical takeoff, horizontal cruise, and vertical landing. By defining velocity profiles from assumed vehicle top speeds and vehicle accelerations, the forces and thus power requirements at each timestep in the flight simulation were determined. To find the forces acting on the aircraft, the software package OpenVSP was used to determine lift and drag coefficients. It was determined that a cruise speed of 264 km/h would generate a lift force equal to gravity, allowing the VTOL propellers to be completely turned off during cruise. Based on this cruise speed, the trip can be completed in just under 38 minutes. The simulation output resulted in a peak power for the VTOL motors of 560 kW, a peak power for the forward motors of 107 kW, and a total power consumption of 94.3 kWh. There are 8 VTOL motors and 2 forward motors. Using the simulation outputs, potential designs were suggested that utilize 350 kW, 250 kW and 150 kW turbogenerators, respectively. The turbogenerator operates at a constant power output to maximize efficiency, and the lithium-ion batteries cover fluctuations in power output. The resulting degrees of hybridization, power system weight, and battery power consumption for each initial design option are summarized in Table 6.

After presenting these findings to the client, the 250 kW turbogenerator design was chosen. The final design includes three different power strategies that can be implemented on the same aircraft. The first option had the turbogenerator on for the entire flight and fully recharged the batteries during the 33-minute cruise. The second design does not consider recharging and leaves the turbogenerator on for the entire flight. The final power strategy option would turn the turbogenerator off for the cruise phase of flight to reduce emission and utilize surplus battery capacity. The results of these three power strategies are summarized in Table 10. These power strategy options highlight the tradeoffs between downtime, degree of hybridization, and fuel consumption. The location of refueling stations, trip demand, and the life cycle of vehicle components must be considered when choosing a strategy, which is why the three options were presented to allow the client greater flexibility. Although three options are being presented, the option being recommended has a degree of hybridization (defined as $\text{battery energy} / [\text{battery} + \text{fuel energy}]$) of 17.8%, a power system mass of 683 kg and requires less than 14 minutes of downtime between flights for charging and refueling.

Table of Contents

1. Background and Introduction	1
2. Scope.....	2
3. Research Summary	3
Batteries.....	3
Turbogenerator.....	3
Electric Motors.....	4
Propellers	5
Vehicle Layout and Stability Considerations.....	6
4. Customer Requirements and Engineering Specifications	6
Customer Requirements	6
Engineering Specifications	7
5. Component Selection.....	9
Batteries.....	9
Turbogenerator.....	10
Electric Motors.....	11
Propellers	11
6. Lift and Drag.....	12
7. Simulation	13
Formulation and Governing Equations.....	13
Simulation Assumptions	17
Turbogenerator Sizing.....	17
Battery Pack Sizing	18
Battery Recharging.....	20
8. Simulation Results.....	20
Sensitivity Analysis	23
Environmental Considerations of Simulation	24
9. Aircraft Stability Analysis	25
10. Final Design	26
Power Strategy.....	26
Bill of Materials	27
Environmental Impact.....	29
Vehicle Comparison	29
Cost Analysis	30
Final Recommendation	31
11. Future Work	31
12. Conclusion.....	32
Appendix A – QFD	35
Appendix B – Weighted Evaluation Matrices	36

List of Figures

Figure 1: Schematic diagram of a series hybrid power system.	1
Figure 2: Upper left: TF-2.0 Lift + Push [1]. Lower left: SureFly multirotor [2]. Right: VA-X4 air taxi [3].	2
Figure 3: Left, standard aircraft propeller configurations, from [9]. Right, a VTOL concept with wing embedded propellers.....	5
Figure 4: Dimensions of the fuselage, with the red area representing the area where no components can be placed.....	6
Figure 5: Coefficients of the moment about the aerodynamic center, lift, and total drag versus angle of attack.	13
Figure 6: Example velocity profile for the forward velocity of the aircraft over the mission duration.....	15
Figure 7: Forces acting on the aircraft at each stage of flight.	15
Figure 8: Schematic diagram of the battery pack and electric motors.....	19
Figure 9: Flight simulation power usage per propellor over duration of the flight.....	21
Figure 10: (Left) Power versus DOH. (Right) Energy efficiency for the three different options.	22
Figure 11: Sensitivity analysis of mission parameters on total energy consumption.....	23
Figure 12: (Left) Example AOA vs. Moment Coefficient plot found using VSPAERO. (Right) Standard aircraft coordinate system.....	25
Figure 13: Final power system component layout and propeller placement.....	28

List of Tables

Table 1: Customer requirements with weighting and justification.	7
Table 2: Engineering specifications with target and justification for the target.	8
Table 3: Pseudo code for the velocity profile algorithm with explanatory text.	14
Table 4: Pseudo code for the power calculations with explanatory text.	16
Table 5: Mission parameters and simulation output from Python simulation.....	20
Table 6: Results from the 3 design options chosen with the two different power strategies.	22
Table 7: Charging information for the different design options and power strategies.....	23
Table 8: CO2 Emissions for Three Design Options.....	24
Table 9: Comparison of various aerodynamic stability parameters given varying battery positions within the aircraft	26
Table 10: Results for the 3 different power strategies presented for the 250 kW turbogenerator design.	27
Table 11: Bill of materials for the final design.	28
Table 12: CO2 Emissions for three 250 kW Power Strategies.....	29
Table 13: Comparison of emissions and trip times of similar vehicles the UAM aircraft.....	30
Table 14: Operation cost for three design options.....	30
Table 15: Weighted evaluation matrix for the 3 different battery options.....	36
Table 16: Weighted evaluation matrix for the 3 different electric motors.	36
Table 17: Weighted evaluation matrix for the 3 different VTOL propellor configurations.	36

1. Background and Introduction

With the quickly growing world population, existing transport infrastructure in and between urban centers cannot suffice to keep up with demand for civilian and commercial purposes alike. Limited space for commercial, industrial, and residential infrastructure means that urban centers are constantly expanding their area. This leads to longer commute times, roadway congestion, and increases the consumption of fossil fuels. Urban air mobility (UAM) is one potential solution. These small aircraft utilize vertical takeoff and landing (VTOL) which eliminates the need for the large infrastructure of traditional airports. Further, UAM would increase trip times and reduce the load on current transportation options. UAM is also not limited to roadways, and vehicles are not limited by travelling at a given elevation. This essentially eliminates traditional transportation congestion problems.

The Structural and Multidisciplinary System Design Lab (SMSD) at Queen's University has begun preliminary design of a UAM vehicle. SMSD has yet to do in-depth power system research and has therefore requested the development of a hybrid power system. The requirements set by SMSD state that the hybrid power system design must enable vehicle travel of at least 150 km and the power system mass must not exceed 700 kg. The final design will feature a vertically and horizontally placed propellers, and all components must be capable of being produced with currently available technology. The vehicle will feature 8 propellers purely for lift/vertical motion, and 2 others for horizontal motion.

The power system will be a hybrid, meaning that the electric motors will be powered by more than one source. Most modern hybrid vehicles use a combination of fossil fuels and electrical power as the two sources of power, most commonly in the form of internal combustion engines and battery packs. There are three different types of power system configurations in modern hybrid vehicles: series, parallel, and series-parallel. In the series configuration, the engine is connected to a generator where shaft work is converted to electrical energy. This electrical energy can then be used to power an electric motor or be stored in batteries. The motor can be powered by a generator, battery storage, or both. This depends solely on the power demand. In the parallel configuration, instead of powering a generator, both the combustion and electric engines are coupled to the propulsion systems. The series-parallel configuration works similarly to the parallel configuration but instead, some of the mechanical energy is converted to electrical energy by a generator and is fed to electrical power storage. Based on the request from SMSD, a series hybrid power system will be developed. A schematic diagram of the system is shown in Figure 1.

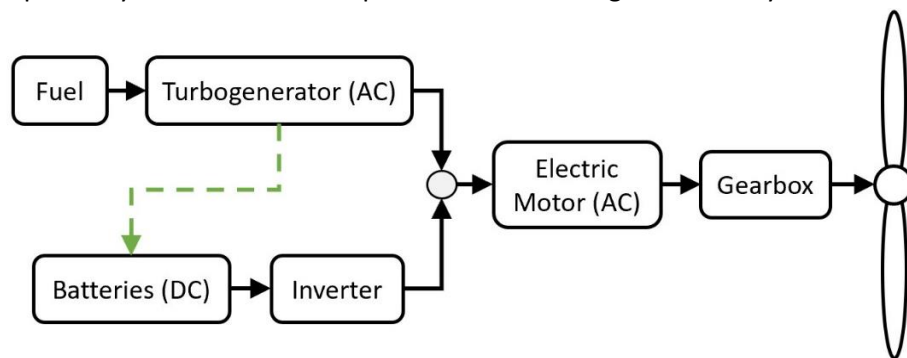


Figure 1: Schematic diagram of a series hybrid power system.

The two sources of power connected to the AC motor are the AC turbo generator, powered via fossil fuels, and DC battery pack, which is converted into AC with the use of an inverter before being routed into the

electric motor. Additionally, as indicated by the green arrow, excess power from the turbogenerator can be routed to the inverter to recharge the battery pack when they are not being used.

Many companies are in the process of developing this technology and there is expected to be a strong market for the product. Terrafugia Corporation has proposed a design for the TF-2.0 Lift + Push. The hybrid power system plans to use 4 lift propellers and 1 cruise propeller [1]. The expected cruise speed is 222-240 km/h with a range of 315-400 km [1]. The aircraft is expected to have a payload of 410-500 kg or 4 passengers with an anticipated operational cost is \$400 per hour [1]. The SureFly is a multirotor hybrid electric design recently purchased by Moog Incorporated. The Surefly utilizes a gas combustion engine for generating electricity, with a battery pack in parallel [2]. It utilizes 8 electric propellers, has an expected range of 70 miles, a top speed of 70 mph, and a maximum payload of 400 kg [2]. The expected selling price is \$200,000 [2]. SureFly achieved the first manned flight of a hybrid-electric VTOL aircraft and is awaiting FAA-type certification [2]. The 250 VA-X4 air taxis from Vertical Aerospace are expected to be certified by 2024 and are being leased by Brazilian airline Gol [3]. The operating cost is expected to be \$1 per passenger for a 25-mile trip [3]. The aircraft is expected to carry 5 people at speed of 322 km/h with a range of 161 km [4]. This aircraft is fully electric with 4 tilt propellers. Despite not being a hybrid UAM vehicle, the V4-X4 will occupy the same market as the intended design. Renderings of the three different designs are shown below in Figure 2.



Figure 2: Upper left: TF-2.0 Lift + Push [1]. Lower left: SureFly multirotor [2]. Right: VA-X4 air taxi [3].

2. Scope

The team has specified and designed components for a hybrid power system suitable for the existing UAM vehicle developed by SMSD. The client has received:

- Mathematical models with associated Python simulation used for component selection, battery sizing, generator sizing and determining required fuel for the aircraft.

- A bill of materials containing all major system components (i.e., fasteners and minor components were omitted) required for the power system.
- A CAD model containing the layout of major components within the existing fuselage (supplied by SMSD).
- OpenVSP model used to determine aircraft stability, aerodynamic coefficients, and center of gravity.

3. Research Summary

The key findings for each subsystem are summarized below.

Batteries

A critical component for battery selection in aviation is specific energy (power density). Lithium-ion batteries have one of the highest specific energies of current batteries, ranging from 100-265 Wh/kg [5]. Lithium-ion batteries are suitable for high power applications, have no charge memory, and have a low self-discharge of 1.5-2% per month [5]. Many electric cars use lithium-ion batteries, and they appear to be the best choice for use in aviation. There are many new types of batteries in development that promise higher power densities, but this tech is a few years away. Industry leaders suggest that a specific energy of 350-400 Wh/kg is needed until the electric aviation industry takes off [6]. Another important aspect is the battery cycle life and possible failure modes. Lithium-ion batteries are typically rated for 200-500 charge/discharge cycles and can be fire risks, especially under high voltage, high temperature, and adverse weather conditions [7]. Thermal runaway is a common issue with batteries and occurs when the rate of heat generation exceeds the rate of heat dissipation. If thermal runaway occurs in one battery cell it can impact adjacent cells and cause a chain reaction that can lead to fires, which is why the batteries must be kept in a climate-controlled area. Battery discharge rate is important when selecting electric motors to ensure the battery supplies enough current. For example, if a battery has a capacity of 10 Ah and a discharge rate of 5C, it can supply a maximum current of 50 A. It is worth noting that the power density rating for batteries is on a cellular level. The total battery and its enclosure will have a lower power density than the values presented above.

Turbogenerator

Gas turboshaft engines are typically used for rotor aircraft vehicles or applications requiring a lightweight and powerful engine. These gas turbine engines differ from jet engines by providing power in the form of shaft work which can directly drive a vehicle or spin a rotor/generator. The UAM series hybrid application will require a direct connection to a generator. Typical applications include helicopters and military land vehicles. On a larger scale, these turboshaft engines are used for industrial power generation. Turboshaft engines are comprised of a compressor or multiple compressor stages and rotating vanes that act as nozzles. These compress the flow of air before a combustor, which introduces and burns aerosolized fuel, increasing the pressure, temperature, and available energy in the fluid. This flow then travels through a turbine stage or multiple turbine stages which act as diffusers and lower the pressure of the flow extracting the energy available. The turbines are connected directly to the compressor stage or stages to power it, forming a feedback loop controlled by throttling the fuel.

Small turboshafts typically have a power-to-weight ratio of 2.0 or above making them valuable for small aircraft [8]. Typical small turboshaft engines produced by Rolls Royce, Turbomeca, and RR Allison weigh

from 61 kg to 124 kg and have shaft power of 186 to 560 kW [8]. These gas turbine engines are small and powerful, as they are used to power rotary-wing aircraft.

Multiple factors come into play for gas turboshaft engines. Most importantly, power to weight ratio, mass, pressure ratio, and efficiency. Typically, larger turbines are more efficient as they operate at higher pressure ratios with multiple stages. To improve efficiency, compressors have multiple stages. The compressor and turbine stages are designed to reduce the change in pressure by small increments per stage. Consequently, this requires more space and adds mass, therefore smaller turbines may have a large power to weight ratio or good efficiency but usually not both. Larger shaft power output units can achieve relatively high-power output for a given mass and efficiency. Most commercial aviation giants offer turboshaft engines in addition to their traditional turbofan and turboprop offerings. This technology is mature and tested, however has not been used for hybrid electric flight.

A traditional generator is a device that converts mechanical energy from an external power source and produces electrical energy as its output. For the UAM vehicle design, the external power source will be a gas turboshaft engine and the electrical output will be used to recharge the batteries or power the electric motors. The output shaft of the turboshaft engine will be connected to the shaft of the generator where magnetic flux is produced generating a voltage [9]. This power generation system via a gas turbine is identified as a turbogenerator. UAM companies have begun to develop the power system for these vehicles for both cargo transport and passenger transport applications. For reference, some American aerospace companies, such as Honeywell, have begun producing aviation-grade generators with power capabilities up to 1 MW [10]. This power rating is more than enough for the SMSD UAM vehicle application. For comparison, Pratt & Whitney, another American aerospace company designs turbo engines used for helicopter applications that can produce 1000 hp (745 kW) [11]. Given that the UAM vehicle is expected to be significantly lighter than commercial helicopters and needs approximately 520 kW (provided by SMSD) of peak power to execute a vertical takeoff, current turbogenerator manufacturing companies will be able to power the UAM vehicle being designed.

Gas turbine engines and consequently turbogenerators operate at the lowest specific fuel consumption (SFC) at the quoted power output. Aerospace applications for propeller or rotary-wing aircraft change the pitch of the propellers or rotors to reduce power while maintaining load. SFC increases at low load due to low thermodynamic cycle and compressor efficiency [12]. Therefore, to maximize efficiency, the turbogenerator should be run as close to the quoted maximum power output as possible.

Electric Motors

An electric motor converts electrical power into rotational mechanical energy. There are several types of electric motors and their power, efficiency and subsequent purpose vary between each type [13]. For this design, the electrical power supplied by the generator and batteries will be used for lift during takeoff, cruise, and landing, as well as forward thrust during cruise. For VTOL, a minimum 65 kW (provided by SMSD) power requirement is needed per motor and the diameter of the motor needs to be kept to a minimum to be able to fit under the vertical facing propeller. For this design, an axial flux motor will be used. Contrary to a radial flux motor, an axial flux motor induces electric fields along the axis of the shaft to which a disk-shaped rotor with powerful alternating-pole magnets is attached [14]. While not a new technology, the axial flux motor was traditionally used as a low-profile, low-power alternative to the radial flux, however, the recent breakthroughs with magnetism and composite materials allowed the creation of powerful and more compact axial flux motors. The advantage of axial flux is it provides large amounts

of power and torque, even at high RPM, and has a relatively low profile. The disadvantages include high torsional loads on the motor, as well as the inertial forces due to the large diameter of the rotor.

Propellers

This research summary aims to explain the relevance of high-level parameters, such as propeller diameter and location, to the design of the aircraft. Generally, as propeller diameter increases, the efficiency also increases [15]. The limitation of the length is maintaining a propeller tip speed which should remain subsonic [15]. The number of blades on a propeller will increase the maximum power output, but the efficiency will decrease due to the increased mass [16]. Thus, after considering total power requirements, the number of blades should be minimized to ensure the highest propeller efficiency. Multiple factors impact the placement of propellers in standard aircraft, and additional factors to be considered when designing for VTOL. For the forward-facing propellers, two main configurations are widely used: tractor or pusher configuration. Some pros to the tractor and pusher configurations are listed below. These points are summarized from section 10.4 of [15].

Tractor:

- Puts engine (electric motor) upfront, which means a smaller tail area is needed to balance the aircraft due to a larger moment arm. This aids with stability.
- The propeller faces undisturbed air, maximizing the efficiency of the propeller.

Pusher:

- A rearward propeller does not disturb the air passing over the fuselage, thus skin friction drag increases, and airfoil efficiency decreases. This reduces required cruise power.
- A layout such as the wing-mounted pusher can enable a reduction in aircraft wetted area by shortening the fuselage. The inflow (and energy added to air) from the propeller allows a much steeper fuselage closure angle without flow separation than otherwise possible.

These considerations are most relevant to standard aircraft, and for a VTOL aircraft, these considerations are only relevant for the forward-facing propellers. For the vertical facing propellers, those which will provide the aircraft's vertical takeoff capability, the most important factor is that the thrust is easily balanced during takeoff. This means that the moments about the center of gravity (CG) must be zero, which will be discussed in the section Vehicle Layout and Stability Considerations. Two common methods of mounting propellers in a VTOL aircraft are via booms, an example of which can be seen in Figure 2 or placing the propellers within the wing. Wing-embedded propellers and some examples of tractor and pusher propellers are shown below in Figure 3.

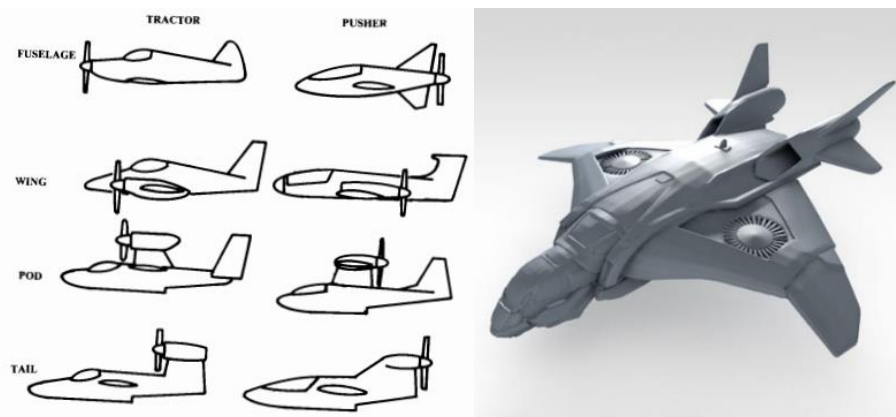


Figure 3: Left, standard aircraft propeller configurations, from [9]. Right, a VTOL concept with wing embedded propellers.

While wing embedded propellers can assist with packaging and maintaining minimum volume, they significantly reduce the effectiveness of the wings as aerodynamic control surfaces. Boom mounted propellers allow the aerodynamic control surfaces to remain largely undisturbed by the propellers, but additional mounting structures are needed which require more mass and design space [17] [18].

Vehicle Layout and Stability Considerations

In a traditional, non-VTOL airplane, longitudinal aerodynamic balance is achieved by balancing the lift forces from primary wings, stabilizers, etc. about the center of gravity. This is practically achieved by adjusting the trim of the horizontal stabilizer to offset the pitching moment created by the lift force generated by the primary wings [15]. The vertical stabilizer performs a similar function, adjusting to compensate for disturbances that generate a yaw moment, such as a crosswind. In a VTOL aircraft, during takeoff and landing longitudinal stability cannot be achieved through trim adjustment of the horizontal stabilizer. The forward airspeed is little, if not zero, resulting in small aerodynamic lift forces. Balancing the moments about the CG in VTOL is achieved with thrust balance. By running the front and rear propeller motors at varying RPM the required thrust can be generated to balance the aircraft. Additionally, paired propellers should be counterrotated to counteract the gyroscopic effect.

In addition to rotor placement, the other components of the power system discussed above must be placed mindfully to ensure forces can be balanced about the resulting CG location. Fuel tank placement is a very important design consideration – as the fuel tank will drain during flight, an improperly placed fuel tank can result in a largely varying CG throughout the flight, which is problematic for maintaining vehicle stability [15]. The fuel tanks must be placed such that the vehicle CG does not vary significantly from its full to empty state. In-depth stability analysis considering mass placement is discussed in Aircraft Stability Analysis.

4. Customer Requirements and Engineering Specifications

Based on the research above and the conversations with SMSD a list of customer requirements and engineering specifications were created to guide the design process.

Customer Requirements

SMSD has provided a layout of the fuselage indicating where components can and cannot be placed, which must be adhered to. The layout is shown below in Figure 4.

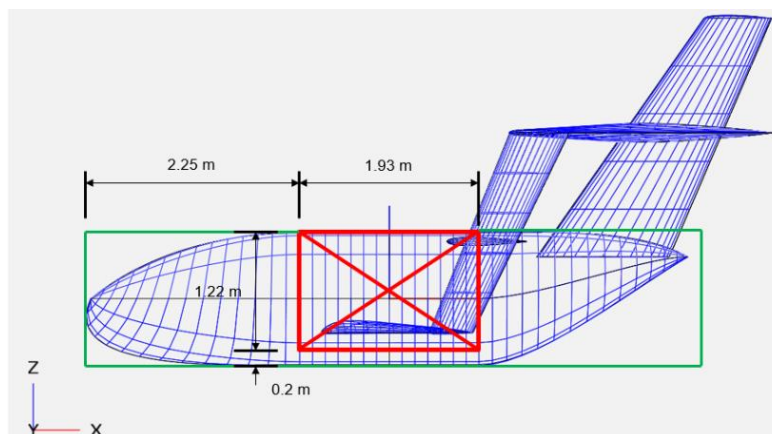


Figure 4: Dimensions of the fuselage, with the red area representing the area where no components can be placed.

Additional customer requirements are listed below in Table 1. One hundred total points were allocated between the customer requirements to create a percentage weighting for importance. Note that the customer requirements have been determined from the perspective of SMSD, an R&D group, and not from the perspective of the end user.

Table 1: Customer requirements with weighting and justification.

Customer Requirement	Weighting (%)	Justification
Quiet Cabin	7	To ensure a pleasant experience for passengers the cabin noise must be kept to a minimum.
Long Range	18	The vehicle is being designed for intercity use; thus, the vehicle must have an adequate range for this purpose.
Lightweight	18	A lightweight design is important in aviation and will result in considerable energy savings, and a larger possible payload.
Low Cost	7	The price is not a critical element of the design due to this being a preliminary design, in addition to the anticipated large market size.
Fast	11	The aircraft speed is related to how many trips per day can be completed and will change the required power output, battery capacity and fuel tank required.
Minimal Carbon Footprint	10	The purpose of the design is to create a more environmentally friendly solution to current aviation, through the use of battery and renewable energy sources.
Manufacturable	6	Due to the early stages in the design, this criterion is not essential, but it is good to consider when making decisions.
Minimal Component Volume	10	All components must fit in the specified design spaces indicated in Figure 4. The minimal component volume will allow more flexibility with component layout and will make stabilizing the aircraft easier.
Long Life Cycle	13	The life cycle will be important for the vehicle to become an economically viable solution.

In addition to the requirements listed in the table above, safety was another important aspect that was addressed with the design. The component selection and vehicle layout focused on minimizing the potential risks involved, namely the battery failure modes and the stability of the aircraft.

Engineering Specifications

A list of engineering specifications with quantifiable targets was created to help meet the customer requirements identified above. The relationships between the customer requirements and engineering specifications are identified in the Quality Function Deployment (QFD) and can be found in Appendix A. The QFD helped to determine the relative importance of each engineering specification, based on the customer requirements, and ensured efforts were appropriately prioritized. The engineering specifications are listed below in Table 2.

Table 2: Engineering specifications with target and justification for the target.

Engineering Specifications	Target	Justification
Cabin Noise	< 70 dB	Cabin noise will come from the power systems and the vibration of the aircraft. The noise must be kept to a minimum to ensure a comfortable ride for future customers. 70 dB is roughly equivalent to a car driving 100 km/h.
Vehicle Range	> 150 km	A minimum travel distance of 150 km is required to provide sufficient intercity travel. However, the point-to-point travel is not representative of the total travel distance, which will be larger due to vertical take-off and landing.
Power System Weight	< 700 kg	MTOW is 1800 kg broken down as 600 kg for structure, 500 kg for payload, and 700 kg for power (supplied by SMSD).
Thrust Balance	The sum of moments about CG is zero	The propellers must be placed such that the moments can be balanced about the center of gravity of the vehicle. If this is not the case the vehicle will pitch/roll/yaw constantly.
Total Cost	< \$1,000,000	A maximum budget has not been provided; however, a more inexpensive model is ideal for the client. A higher budget limit is initially set for this prototype.
Payload	> 500 kg	Based on the mass breakdown provided by SMSD the required payload is 500 kg.
VTOL Power	520 kW	The vehicle has 8 vertical propellers that provide approximately 65 kW of vertical power each (provided by SMSD). The vehicle must be light enough to achieve the vertical take-off and landing with the provided power.
FW Power	108 kW	2 forward propellers provide approximately 54 kW of power each (provided by SMSD). 2 FW propellers will provide thrust during cruise to maintain the desired cruise speed of 110 km/hr.
Degree of Hybridization	50% of Power from Fuel	To minimize the environmental impact of the vehicle, a goal of a 50% degree of hybridization was set.
Flight Stability Performance	Stability coefficient < 0	The stability coefficient must decrease with an increasing angle of attack and vice versa. This ensures that the vehicle recenters itself after a disturbance.
CG location and consistency	< 5% variation in location	A consistent center of gravity location enables stable handling characteristics of the aircraft throughout its flight.
Fuel/Battery Capacity	TBD based on simulation	The fuel and battery capacity will determine the range and payload the vehicle can carry. The target value will be determined once the simulation had been completed.

Based on the QFD analysis, the most important engineering specifications are fuel/battery capacity, power

system weight, and vehicle range. There are many tradeoffs between the engineering specifications identified in the QFD. For example, increasing the fuel/battery capacity will increase the vehicle range, but it will also increase the power system weight, which will decrease the range. There is another tradeoff between the total cost of the power system and the VTOL and FW power. Adding more power will help increase the payload and potentially the range but will be more expensive and likely increase the mass of the design. Aircraft design is full of tradeoffs, which is why the computer simulation developed was such a critical tool for the power system design. The simulation created a better understanding of the many tradeoffs involved in the design and provided a tool for validating component selection.

The three competitors discussed in Background and Information were assessed against the customer requirements in Table 1 to determine where the intended design can best fit into the market. Due to limited information on competitors, best judgment was used when ranking the competitors against the customer requirements. When no reasonable assumption could be made, a neutral score of 3 was given.

5. Component Selection

The power system was broken down into five main components: batteries, gas turbine, generator, electric motors, and propellers. A weighted evaluation matrix (WEM) was used for component election when necessary. Unique design criteria were chosen for each component based on research and customer requirements to determine the best option. Once the criteria were chosen for each component, each team member voted on what they felt the weighting should be. The mean and standard deviation were calculated for each weighting with the error being propagated through to the final value. Options are ranked relative to one another, a 3 represents the best option and 1 the worst. If detailed information could not be found for a certain criteria or option, a general ranking of low (1), moderate (2), or high (3) was used. The option with the highest total value represents the best option. The uncertainty in the final value provides the confidence with which that option can be chosen.

Batteries

Three different lithium-ion battery options were compared using six different criteria: cost, specific energy, specific power, safety, performance, and cycle life. Specific energy is given in Wh/kg and relates to the runtime of the battery. Specific power is related to the battery's ability to deliver a high current. Note that there is a tradeoff between specific power and energy, a high current will decrease the runtime of the battery and a low current will increase the runtime. Safety relates to the issues of thermal runaway in batteries and the temperature at which this process begins for each cell type. Performance relates to how well the battery performs at different temperatures and will determine the amount of climate control needed for battery storage. Typically, batteries will degrade faster at high temperatures and the capacity is temporarily reduced at low temperatures [19]. Cycle life is related to the number of charge and discharge cycles the battery can undergo before needing to be replaced.

The first is a lithium nickel manganese cobalt oxide (NMC). NMC is commonly used in electric powertrains and electric vehicles due to its low cost and high specific energy [19]. Another benefit of NMC is the cells can be optimized for specific energy or power [20]. The cost of NMC's is estimated at \$350/kWh, with a cycle life of 1000-2000 and a thermal runaway temperature of 210°C [3]. They have relatively high specific energy at 150-220 Wh/kg and a moderate specific power [3]. NMC's have moderate performance in various temperatures compared to other lithium-ion cells [3]. The second option is a lithium nickel cobalt

aluminum oxide (NCA). NCA's have the highest specific energy of the options compared but this comes at a lower level of safety [19]. The specific energy is 200-260 Wh/kg, and the specific power is moderate compared to the other lithium-ion options with a discharge rate of 1C [3]. The cost is estimated at \$420/kWh and the expected life is 500 cycles [3]. Thermal runaway occurs at 150°C and the performance is rated as moderate [3]. The third option is lithium titanate (LTO). LTO's have a specific energy of 50-80 Wh/kg and cost \$1,005/kWh [3]. The high cost and low specific energy are offset by the strong performance in the other four criteria and their fast-charging rate. LTO's have high specific power, with a discharge rate of 10C, and are rated for 3,000-7,000 cycles [3]. They are one of the safest lithium-ion options with high thermal stability and excellent low-temperature properties, able to maintain 80% capacity at -30°C [3]. All three options were compared using the WEM in Table 15 of Appendix B.

Based on the results of the WEM, the NMC battery was the most suitable choice moving forward, although it was not outside the range of uncertainty of the LTO. This was primarily a result of its strong performance in the specific energy criteria, which was deemed the most essential for the design. The LTO battery was a very close second because it scored very well on secondary features such as safety, performance, and cycle life. The difference in the NMC and LTO highlights the tradeoff that exists in battery technology between specific energy and specific power. One thing that should be mentioned is the relatively low weighting given to performance. An airplane will be subject to a large range of temperatures, but it is assumed that for safety, regardless of the battery chosen, a temperature control system will be required.

With the specific type of lithium-ion cell selected, it was determined that the Grepow NMC811-20 would be the most suitable model. The Greypow battery is suggested for UAM, and VTOL applications, plus it has higher specific energy than other comparable batteries [21]. A single battery has a capacity of 20 Ah, a discharge rate of 5C, a charge rate of 1C, and a cell voltage of 22.2 V. The mass of a battery is 1.8 kg and has a volume of 189 x 76 x 58 mm [21]. The battery is capable of maintaining 90% of its capacity after 600 charge-discharge cycles and is rated for a depth of discharge (DOD) of approximately 90%, meaning that 90% of the available battery capacity can be utilized [21]. All this information is for a single battery. For the actual design, a battery pack will need to be designed that meets the power requirements of the aircraft, which will be determined below.

Turbogenerator

After completing the research on the generators and turbines currently available on the market today, it was decided that a combined turbogenerator would be implemented. This was due to a lack of specifications found during the research phase of the project as mass was not able to be found for components considered. Another advantage of using a turbogenerator instead of a turboshaft and generator connected together is guaranteed compatibility between components. Therefore, a turbogenerator power output is as quoted by the manufacturer. Generator losses do not need to be accounted for. Honeywell has developed a turbogenerator for their UAM vehicle concept with power capabilities up to 1 MW and is the suggested power source for this application [10]. For the purpose of this design project, it is assumed that Honeywell will be able to supply a turbogenerator with the specific power output that is determined from the simulation. The Honeywell turbogenerators have very limited information available. As a workaround for the lack of available information, the power density was approximated using the power densities of a turbine and generator of the expected size needed. The Rolls

Royce M250 turbine has a mass of 73 kg and a power output of 330 kW [8]. Honeywell produces a 250 kW generator that weighs 33 kg [22]. It is assumed that the power densities can be scaled for different power output levels to find the approximate mass of the turbogenerator at various power outputs. In practice, the turbogenerator must be specifically designed for a specific power output to ensure maximum efficiency output and therefore, conversations with the supplier will be needed to get exact specifications. At this stage of the design, it was assumed that this approximation would produce adequate results. The turbogenerator will supply a relatively constant power supply during flight to allow it to operate at higher efficiencies.

Electric Motors

For this project, the power requirement per motor as provided by SMSD is roughly 65 kW. Other considerations for choosing the motors include mass, continuous and peak power, maximum speed (RPM), and size/profile. Because the technology is quite new and still being developed, the cost of the motors is quite variable and will not be one of the primary considerations. Three different electric motor options are compared in Table 16 of Appendix B.

Each motor has a very similar profile, in a disc-shaped composite material casing. The casings vary in thickness and most importantly diameter. The size consideration was drawn primarily off of the diameter of the casing as the thickness varied little between the motors. The mass of the YASA P400 R and the EMRAX 268 was quite similar and both motors were significantly lighter than the EVO AF140. However, the EVO had a significantly higher continuous and peak power output compared to the other two motors. Lastly, the EVO and EMRAX had very similar maximum RPM outputs but were significantly less than the YASA model. However, this could be solved with the use of a gear/gearbox system. Overall, the EMRAX 268 has the higher score in the evaluation matrix, mainly due to its versatility and good performance while maintaining a smaller mass and profile and will be used in the final design [18] [17] [23].

Propellers

Three layouts of the propellers are considered in Table 17. These are wing embedded, boom mounted on the wings, and boom mounted on the wings and fuselage. See Figure 2 and Figure 3 as a reference for the different propeller mounting methods. The propellor layout must accommodate multiple propellers. The lift from the propellers must counteract gravity, to do so, ensuring 8 propellers will easily fit within the assembly is of utmost importance. The design must be capable of stabilizing the aircraft during takeoff and landing. This means that the VTOL propellers must be laid out in a way that the lift vectors from each motor will not cause any pitch, yaw or roll unless it is desired. To make sure that cruise is as efficient as possible, it is important that the propellers do not significantly interfere with control surfaces such as the wings and tail. Otherwise, lift and stability provided by these control surfaces will be lost. Last, mass, and total design volume are important to ensuring the propeller system will enable the highest vehicle efficiency, and easily integrate with the other components. The WEM used to evaluate the different options is shown in Table 17 of Appendix B. It is concluded that boom mounting on the wings and fuselage will be necessary for the UAM design. Placing the propellers on the wings and throughout the fuselage allows thrust balance to be achieved without relying on large power differentials (caused by short moment arms), which can be unstable. Boom mounted propellers on the wings/fuselage will be at the expense of mass and design volume; however, the alternative options are less in favor of stability, which is not ideal for a VTOL aircraft.

A fixed-pitch natural-composite propeller from MT-Propeller has been selected. MT-Propeller custom builds fixed pitch propellers depending on specific customer requirements, however, the propellers can accommodate engine powers of 40 – 400 HP (29.8 – 298.28 kW) and diameters of 1.2 m to 2.5 m [24]. Given the SMSD provided diameter of 1.5 m, and a peak power of approximately 65 kW, these propellers will be suitable for usage in the final design. Furthermore, at a density of only 0.7 g/cm³, the propellers are estimated to have a mass of 4.15 kg as per the mock propeller made in SolidWorks. This CAD does not include fasteners or other potential mass increasing components; thus, the mass is likely an underestimate. The number of propellers and the pitch angle will need to be decided in a future power system iteration. Properly selecting these parameters would require in-depth aerodynamic analysis, which was not feasible given the scope of this project. The team wanted to primarily investigate design variables directly related to the sizing of energy-storing/producing devices in this project. However, for future research, the effects of number of blades and pitch angle on total power output and propeller efficiency should be investigated further.

6. Lift and Drag

The forces created by the aerodynamics of the UAM vehicle were critical in creating the flight simulation which was used for component selection and validation. Given that the UAM model has multiple wings, an in-depth aerodynamic analysis would consider how the flow of air interacts between the multiple wings. This interaction was not investigated significantly due to the timeline of the project. Instead, the aerodynamics analysis was strictly done in the OpenVSP paired with VSPAERO software. The aerodynamic analysis did not include the impact that the propellers have on the aerodynamic performance, only the aircraft body was considered. This was outside the scope of the project but is something that should be considered in the future. The ultimate goal of the aerodynamic analysis was to determine the lift and drag coefficients of the aircraft, which are needed to find the force and power required for flight.

The coefficients of lift and drag are properties that must be experimentally determined. The experimental analysis was completed using the OpenVSP and VSPAERO software. A model of the UAM vehicle was provided by the SMSD team for this analysis. The software required an input of a Mach number for flight speed to assist in determining the coefficients of lift and drag. Initially, the lift and drag coefficients were found using the suggested cruise speed provided from SMSD of 150 km/h. These values were then inputted into the simulation, which determined the resulting force and power required by the VTOL and FW propellers. The simulation determined that the power requirements would be greatly reduced by increasing the cruise speed so that the force of gravity would be balanced by the lift force, eliminating the need for the VTOL propellers during cruise. This resulted in an increase in cruise speed to 264 km/h (73.3 m/s) and will be discussed further in the Simulation section of the report. An iterative approach was used between the simulation and OpenVSP to make sure the lift and drag coefficients resulted in a cruise speed in the simulation that matched the Mach number being used in OpenVSP. Based on the cruise speed of 73.3 m/s, the Mach number was determined using Equation 1, where c was the speed of sound at 615m altitude and 20°C of 338 m/s [25].

$$Ma = V/c \quad (1)$$

A Mach number of 0.2 was then used for the aerodynamic analysis. Running the OpenVSP software with the UAM vehicle created relationships between the coefficient of lift (C_L), coefficient of total drag (C_{D_Tot})

and the coefficient of the moment about the aerodynamic center along the flight axis (C_{My}) versus angles of attack varying from -10 to 10 degrees. The relationships can be seen in Figure 5.

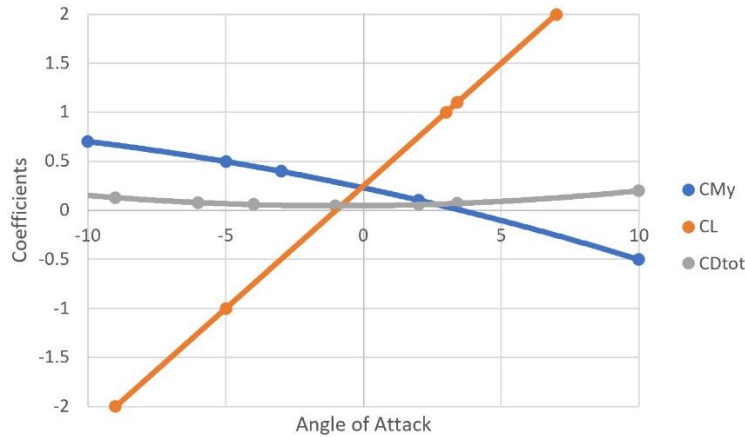


Figure 5: Coefficients of the moment about the aerodynamic center, lift, and total drag versus angle of attack.

The angle of attack for stable flight needed to be determined to model the forces acting on the vehicle during cruise. This angle of attack occurs when the moment about the aerodynamic center along the flying axis of the vehicle is zero. This corresponded to an angle of attack of 3.4 degrees. Using this angle of attack, C_L and C_D were determined to be 1.1 and 0.07, respectively. OpenVSP was also used to find the frontal areas of the aircraft during VTOL and cruise. It should be noted that the angle of attack for cruise was determined using the UAM vehicle alone. The masses for the hybrid power system components were not considered as the total power needed to be determined before component selection. This was necessary as the resulting component masses were dependent on the simulation.

During VTOL, the coefficients of lift and drag needed to be determined as well. Since there was no forward velocity during VTOL, the coefficient of lift was negligible. For simplicity, the coefficient of drag during VTOL was modelled as if the UAM vehicle was a cube. This corresponds to a C_D of 1. This was done since the aerodynamic analysis of the propellers operating along the VTOL axis span a large area but are constantly moving. A more in-depth aerodynamic analysis of the interaction between the VTOL propellers would need to occur to accurately determine the C_D . It is assumed that the cube approximation overestimates the drag on the aircraft, providing an overestimate of the power needed during VTOL.

7. Simulation

Formulation and Governing Equations

To validate the power system component selection, the team created a flight simulation. This simulation outputs the required power for the VTOL and forward-facing electric motors for the entire flight duration, and the total energy required for the entire flight. To create the simulation, the flight was first defined by a set velocity profile. This means that the vertical and forward velocities are provided as inputs to the simulation for any point in the flight. By defining the full velocity profile of the flight, solving for the forces acting on the UAM becomes straightforward. This in turn makes calculating power requirements much easier than attempting to dynamically simulate the aircraft, which would be very complex and outside the scope of this project.

By setting an initial velocity, a final velocity, and an acceleration for the UAM vehicle in both VTOL and cruise, the velocity with respect to time is constrained and thus can be solved for. This was done using kinematic equations, and a process similar to momentum update. The first step is to determine the distance where the specified cruise speed would be reached. Note that for both VTOL and forward travel, a cruise speed is defined, and the term cruise speed will not be used exclusively with respect to forward travel. In the case of VTOL, the cruise speed corresponds to the steady-state velocity in the upwards/downwards direction. In forward travel, the cruise speed corresponds to the steady-state velocity in the horizontal direction. The distance where cruise speed, in either VTOL or forward motion, is reached can be calculated using Equation 2.

$$\text{Distance to Cruise} = \frac{(\text{Specified Cruise Speed})^2}{2 * \text{Specified Acceleration}} \quad (2)$$

It was assumed that the UAM vehicle would decelerate at the same rate as it accelerated. Therefore, using the distance to cruise speed and the total distance, the distance where the deceleration process must initiate can be defined using Equation 3.

$$\text{Deceleration Initiation Distance} = \text{Total Specified Distance} - \text{Distance to Cruise} \quad (3)$$

Given the distance where deceleration must initiate, a Python code was developed to create the velocity profile for both VTOL and forward motion. The code, given a timestep, loops until the total distance is reached, updating the velocity and distance based upon the inputted acceleration and cruise speed. Pseudo code for this algorithm is outlined in Table 3.

Table 3: Pseudo code for the velocity profile algorithm with explanatory text.

Pseudo Code for Velocity Profile Algorithm	Section Explanation
While distance < total distance specified	Run the code while the distance travelled is under the distance specified.
if distance >= deceleration initiation distance velocity = velocity – (specified acceleration) * dt distance = distance + (velocity) * dt time = time + dt	This section checks at the start of the loop if the deceleration distance has been met. If so, start reducing velocity based on the inputted acceleration.
else if (velocity < specified cruise speed) velocity = velocity + (specified acceleration) * dt	Corresponds to the initial acceleration. While the speed is less than cruise speed, increase the velocity by the product of acceleration and timestep
else velocity = specified cruise speed	If the velocity is greater or equal to the specified cruise speed, set the velocity equal to the specified cruise speed.
distance = distance + (velocity) * dt time = time + dt	Update the distance and time.
time.append(t) distance.append(d) velocity.append(v)	Store the values into arrays.

Although the velocity profiles for VTOL and forward cruise correspond to velocities in different directions, the calculation process to obtain each profile is the same thus the same code is used to create velocity profiles for VTOL and forward cruise. An example plot of the trapezoidal velocity profile for forward cruise is shown in Figure 6.

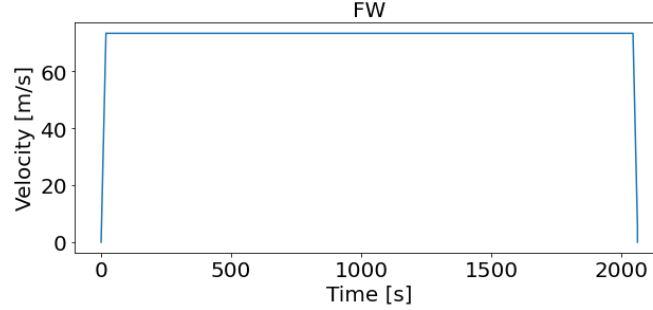


Figure 6: Example velocity profile for the forward velocity of the aircraft over the mission duration

Given that the velocity is now tabulated for all finite timesteps over the entire trip duration, the VTOL and forward cruise power requirements can be calculated. Before discussing the power requirements, the forces acting on the aircraft for each timestep must be identified using free body diagrams. In Figure 7, the forces on the aircraft at each stage in the flight path are identified.

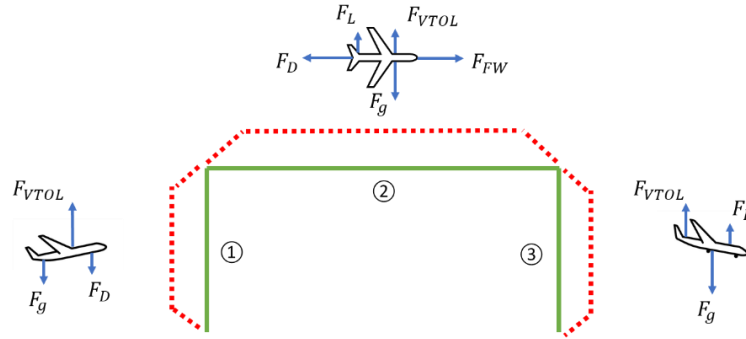


Figure 7: Forces acting on the aircraft at each stage of flight.

Forces acting on the aircraft during VTOL are limited to the vertical thrust and drag forces, plus gravity. In forward cruise, the forces include the lift force from the airfoils, the forward thrust force, the vertical thrust force (if the lift does not meet or exceed gravity), the horizontal drag force, plus gravity. Lift and drag are calculated using Equation 4 and Equation 5.

$$F_D = \frac{1}{2} \rho v^2 C_D A \quad (4)$$

$$F_L = \frac{1}{2} \rho v^2 C_L A \quad (5)$$

C_L , C_D and A were obtained in VSPAERO, as discussed in Lift and Drag. The velocity is known for any point in the flight, as per the velocity profile. Therefore, it is possible to calculate lift and drag for any point in the flight. Given lift and drag plus the mass of the aircraft, the required VTOL and forward thrust forces can be calculated for each by solving $\sum F_x = \sum F_y = 0$. Given the thrust forces acting on the aircraft, the power requirements can be computed. Required VTOL power *per VTOL motor* is expressed in Equation 6 and required power *for all forward motors* is expressed in Equation 7. Power is calculated per motor in

VTOL since the power is dependent on the propeller's radius, whereas forward power is only dependent on the drag coefficient and vehicle velocity which are independent of each propeller.

$$P_{VTOL} = T \sqrt{\frac{T}{A} * \frac{1}{2\rho}} \quad [26](6)$$

Where T is the vertical thrust force per motor, A is the actuator disc area ($\pi * (\text{propeller radius})^2$), and ρ is the density of air.

$$P_{FW} = F_D * v \quad (7)$$

Where F_D is the drag force, and v is the aircraft's horizontal velocity.

Since all variables in Equation 6 and Equation 7 are known, the required VTOL and forward cruise power can be calculated over the entire flight duration. Pseudo code for the algorithm used to calculate required power at each simulation timestep is presented in Table 4.

Table 4: Pseudo code for the power calculations with explanatory text.

Pseudo code for power calculations	Section explanation
<pre> define VTOL_power_func(mass, velocity, Cd) Fg = mass*g Fd_v = 0.5*rho*Cd*Atop*velocity^2 VTOL_thrust = (Fg + Fd_v)/num_VTOL_prop VTOL_power = VTOL_thrust *sqrt((VTOL_thrust /A_prop)*(1/(2*rho))) define Forward_power_func(mass, velocity, Cd) Fg = mass*g Fd_v = 0.5*rho*Cd*A* velocity ^2 VTOL_thrust = (Fg + Fd_v)/num_prop VTOL_power = VTOL_thrust *sqrt((VTOL_thrust /A_prop)*(1/(2*rho))) Fd_f = 0.5*rho*Cd*Afront*v^2 Forward_power = (Fd_f* velocity)/num_Forward_prop </pre>	<p>Function definitions for the power calculations in VTOL and forward (FW) cruise. The FW power function includes the VTOL power calculations as the airfoil lift force can only counteract gravity entirely once the aircraft reaches maximum speed. The landing function is not shown since it is identical to the VTOL_power_func, except for the drag force is subtracted from gravity force since drag opposes gravity on landing.</p>
<pre> for i in range(len(takeoff)) power = VTOL_power_func(mass, velocity, Cd) for i in range(len(forward cruise)) power = FWcrusie_power_func(mass, velocity, Cd, Cl) for i in range(len(landing)) power = VTOL_power_func(mass, velocity, Cd) </pre>	<p>The total trip is split into three sections, takeoff, forward cruise, and landing. These loops will run the appropriate power calculation for the corresponding trip section.</p>

Now the power consumption at any point in the flight can be determined. The integral of the power curve is equal to the total energy consumed throughout the flight. The required electrical input energy is found by considering the efficiencies of the propellers and electric motors. The results of the simulation and the conclusions drawn are discussed in Simulation Results.

Simulation Assumptions

Assumptions made in order to complete the simulation include oversimplification of aerodynamic behaviors, presumed losses, and the velocity profile. Airplane and propeller aerodynamics significantly impact the power requirements of a propeller-driven aircraft. As discussed in Lift and Drag, the aerodynamic lift and drag forces were obtained using VSPAERO. However, a limitation of the VSPAERO model is the lack of propellers and propeller booms integrated into the geometry. These geometry features, if implemented, would change the resulting lift and drag coefficients. Since aerodynamic analysis is not the primary focus of this report, the VSPAERO model geometry was not modified from the geometry provided by the client.

Additionally, the VTOL power equation is derived using highly idealized momentum conservation principles, refer to [26] for more information. While the VTOL power equation is an acceptable baseline for the purposes of this simulation, the use of the equation neglects changes in propeller efficiencies with RPM, and flow around the propeller and how this may affect wing lift/drag.

The usage of a velocity profile greatly simplifies the power calculations. However, utilizing a predefined velocity profile means that the accelerations and top speeds are based upon presumption rather than the aircraft's actual capabilities, which could be limited by many factors outside of power requirements (vibrations, passenger comfort, air braking, etc.). For simplicity, trapezoidal velocity profiles were assumed with constant acceleration. To achieve more accurate results, more realistic velocity profiles should be used.

Turbogenerator Sizing

An important aspect of the power strategy is allowing the turbogenerator to operate at a relatively constant power output with the battery supporting any fluctuations from the baseline power. The power density of the turbogenerator is being approximated using values from a turbine and generator. Equation 8 shows how the mass of the turbogenerator is found based on the required power output.

$$m_{Turbogen} = D_{Turbine}P_{Turbogen} + D_{Gen}P_{Turbogen} \quad (8)$$

Where D represents the power density in units of kg/kW. The simulation works by specifying the desired turbogenerator power output and Equation 8 calculates the required mass. Based on the Rolls Royce M250 turbine, $D_{Turbine}$ is 0.22 kg/kW (73 kg/330 kW) and D_{Gen} is 0.13 kg/kW (33 kg/250 kW) based on the Honeywell generator discussed above in Component Selection. The required $P_{Turbogen}$ needed to achieve the customer requirements is determined iteratively using the simulation. Based on the input mission parameters, the simulation will output a peak power, which will determine the size of the turbogenerator and battery needed. This relationship is expressed using Equation 9.

$$P_{Peak} = P_{Turbogen} + P_{Pack} \quad (9)$$

Where P_{Pack} is the power that the battery can produce and will be discussed below. An additional aspect of the turbogenerator is the fuel mass. The amount of fuel used depends on the efficiency of the gas turbine at the given power output. A common metric used for turbines is specific fuel consumption (SFC), which is similar to miles per gallon rating for a car. There is very minimal information available on the Honeywell turbogenerators, so SFC data from a similar component was used to approximate the behavior.

Honeywell provides an SFC curve for their T53 Turboshift helicopter engine [27]. The curve plots the relationship between SFC in units of lbm/hp/hr, which is equivalent to kg/kWh in SI units, versus power output. The SFC curve from the data sheet was converted to the appropriate units and recreated in the Python simulation, allowing the SFC value to be automatically determined, in kg/kWh, based on the turbogenerator power output selected by the user. The T53 has a larger power output than is anticipated for this design so the values were linearly extrapolated from the provided data.

Another important aspect in calculating the fuel mass is the total energy supplied by the turbogenerator in kWh ($E_{Turbogen}$). Equation 10 was used to calculate the energy from the turbogenerator.

$$E_{Turbogen} = P_{Turbogen}t_{VTOL} + P_{Charge}t_{Charge} \quad (10)$$

The turbogenerator must be on at full power during VTOL, this is when the power demand is the highest. Once at cruise, the turbogenerator power can be reduced or completely turned off if desired, assuming the battery is capable of power cruise alone. P_{Charge} represent the power supplied by the turbogenerator, during cruise while the turbogenerator is on. The charge subscript refers to the time that is spent recharging the battery, which will be discussed below. As an arbitrary example, if the power needed during cruise was 100 kW and 50 kW was needed to recharge the batteries, P_{Charge} would equal 150 kW. If the battery has enough power and energy capacity, it is possible that it could power cruise without the turbogenerator. In the event where the turbogenerator is turned off during cruise, t_{Charge} is equal to the time spent at cruise, which is determined by the simulation, minus the time the turbogenerator is off. If the aircraft were at cruise for 20 minutes, and the batteries have enough capacity to power cruise for 10 minutes, there would be 10 minutes of potential charging time. Both the cruise time and time off are inputs in the simulation used to automatically calculate the charge time. It is worth noting that P_{Charge} can be set to any value and the turbogenerator does not have to be used for charging. Finally, the fuel mass can be calculated using Equation 11, where R is the desired fuel reserve ($R = 1.06$ for this design).

$$m_{Fuel} = (SFC)E_{Turbogen}R \quad (11)$$

The sizing of the turbogenerator and calculation of fuel mass required many assumptions due to the lack of available information. These assumptions should be further investigated if the design is to be implemented and more detailed values can be provided by the supplier once a formal design is proposed.

Battery Pack Sizing

The battery pack sizing is dependent on the peak power required by the aircraft and the baseline power that is being provided by the turbogenerator, as shown in Equation 12.

$$P_{Pack} = P_{Peak} - P_{Turbogen} \quad (12)$$

As discussed, the simulation will output the peak power required during the flight in kW and the user will select how much baseline power they wish to supply using the turbogenerator. Once the battery power is determined the appropriate voltage needs to be found based on the electric motor being used.

The EMRAX 268 comes in low, medium, and high voltage options. All three options have the same mass and have power outputs rated between 40 and 80 kW, which is in the desired range [17]. The data sheet for the motor provides power and current requirements at two different levels of operation, peak power and continuous power [17]. The voltage can be found by dividing the power by the current. The voltage

versus power was plotted in excel and a linear model was fit to the data to produce Equation 13,14 and 15.

$$V_{low} = 0.0006(P_{motor}) + 537 \quad (13)$$

$$V_{med} = 0.0002(P_{motor}) + 461.3 \quad (14)$$

$$V_{high} = 0.0002(P_{motor}) + 166.9 \quad (15)$$

In the above equations, P_{motor} represents the power needed at each motor, which is P_{peak} divided by eight and is in W, rather than kW. It is assumed that the peak power will occur during takeoff when 8 motors are being used rather than only two motors during cruise. The voltage remains relatively constant regardless of power, as seen by the small slope in the equations above. Fluctuations in power requirements are primarily covered by changes in current. A schematic diagram of how the battery pack connects to the motors is shown in Figure 8. The blue squares represent the individual batteries that make up the battery back and the grey circles represent the electric motors.

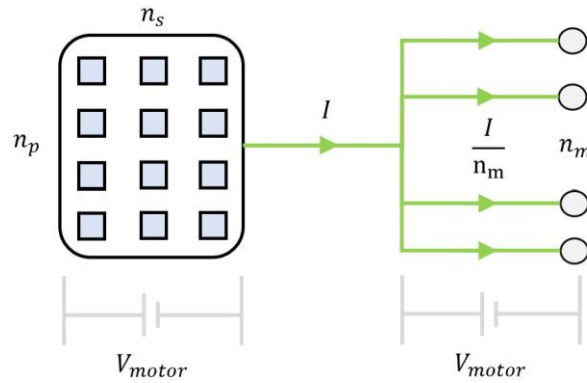


Figure 8: Schematic diagram of the battery pack and electric motors.

The number of batteries in series (n_s) determines the voltage of the battery pack and must meet whatever voltage is found from Equation 13, 14, or 15. The current (I) is controlled by the number of cells in parallel (n_p) and is found by dividing P_{Pack} by V_{motor} . As the power requirement changes throughout the flight the current will adjust accordingly to meet the power demand. The number of cells in series is found by dividing V_{motor} by the voltage of a single battery, which is 22.2 V, this value must be rounded up to the nearest whole number. The number of cells in parallel is found by dividing the total current (I) by the maximum current that the battery can discharge and is also rounded up. The maximum single battery current is the product of capacity and discharge rate, which produces a current of 100 A (20 Ah multiplied by 5C). The total number of cells needed in the pack is the product of n_s and n_p and the total mass is found by multiplying the number of cells by the mass per cell of 1.8 kg. The battery power is split between the electric motors, which are in parallel. The parallel wiring decreases the current, but the voltage remains unchanged, allowing the motors to operate at the correct voltage and each supply an equal portion of the total power. The battery and turbogenerator will be wired in parallel to the electric motors, with each supplying a different amount of power, but the same current (V_{motor}).

Another important parameter of the battery pack is its energy capacity (E_{pack}). The capacity determines the total amount of energy supplied and can be found using Equation 16.

$$E_{pack} = \frac{V_{motor} n_p C_{cell}}{1000} \quad (16)$$

C_{cell} represents the capacity in Ah. The value was divided by 1000 to get into units of kWh. An additional 10% of mass has been added to the battery pack to account for cooling systems. Determining the specific cooling system to be used was outside the scope of this project but is recommended as future work. The simulation automatically computes all this information based on the power requirements of the aircraft and the size of the turbogenerator. The user then chooses the most lightweight battery back, corresponding to the low, medium, or high voltage motors.

Battery Recharging

Battery recharging is an important aspect to consider when minimizing the downtime between possible trips. The time needed to recharge depends on the battery capacity and the suggested charge rate. The Greypow batteries being used have a charge rate of 1C and a suggested charging voltage of 25.2 V [21]. As mentioned above, adding batteries in parallel increases the current, which also increases the capacity. The capacity of the battery pack is the product of the capacity of a single cell (Ah) and the number of cells in parallel (n_p). The voltage needed to charge the battery pack is the product of the voltage needed per cell (25.2 V) and the number of cells in series (n_s). The power needed, in kW, to charge the battery pack is shown below in Equation 17.

$$P_{charge} = IV = \frac{((R)n_p C_{cell})(n_s V_{charge(cell)})}{1000} \quad (17)$$

The voltage must equal the suggested value, but the current can be decreased. R represents the charge rate, which is 1C for the Greypow battery, meaning that if R is set to 1, Equation 17 will provide the power needed to charge the entire battery pack in 1 hour. The amount of energy restored to the battery in kWh can be found using Equation 18 where t is the charge time in hours.

$$E_{Battery} = P_{charge} * t \quad (18)$$

8. Simulation Results

The simulation was run using the mission parameters provided by the customer as inputs. The mission parameters and simulation output are shown below in Table 5.

Table 5: Mission parameters and simulation output from Python simulation.

Mission Parameters		Simulation Output	
Range	150 km	Peak Power - VTOL	560 kW
Cruise Speed	264 km/h		
Cruise Acceleration	0.2 g	Peak Power - FW	107 kW
Altitude	610 m		
VTOL Speed	21.6 km/h	Total Energy	94.3 kWh
VTOL Acceleration	0.4 g		
MTOW (max takeoff weight)	1800 kg	Trip Duration	37.86 min
Power System Mass	~700 kg		

The simulation produces a plot of the power consumption during the flight, shown below in Figure 9. An axis break was added to the middle portion of the flight to allow more detail to be seen in the takeoff and landing sections of the power curves.

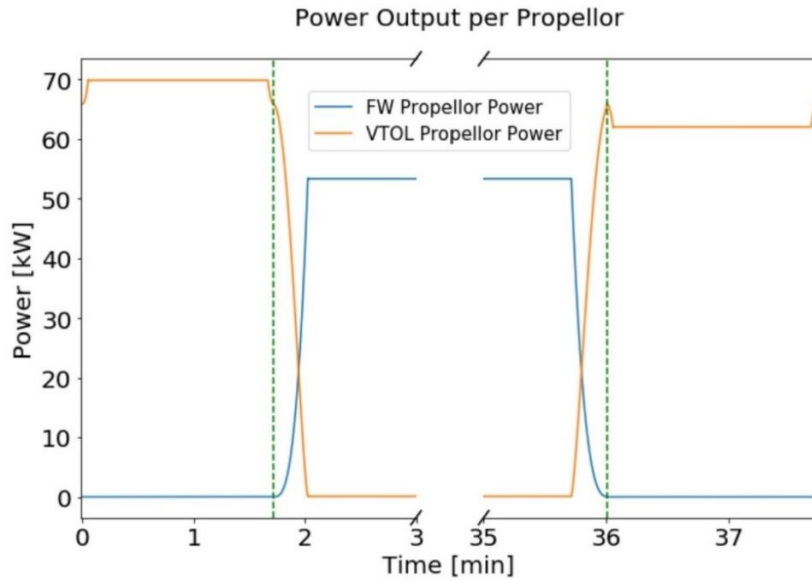


Figure 9: Flight simulation power usage per propellor over duration of the flight.

Figure 9 shows the expected power output at each motor and confirms that the operating range of the EMRAX 238 will be suitable for all 10 motors on the UAM vehicle with both VTOL and FW motors operating primarily between 50 and 70 kW (motor range 40 to 80 kW). The left portion of Figure 9 illustrates the takeoff and shows how the power increases in the VTOL motors while the aircraft accelerates, then once it reaches its accent speed the power output is constant until the aircraft slows down as it approaches the desired altitude. Once the altitude is reached, the forward motors are turned on and the power steadily increases as the aircraft accelerates to full speed. As the speed increases, the lift force generated by the wings increases, which decreases the need for VTOL power and eventually goes to zero once the cruise speed is reached. By turning off the VTOL motors during cruise, significant energy can be saved. The VTOL speed was determined to be the largest contributor to overall power consumption, which is why the cruise speed was increased from the original customer request of 150 km/h to 264 km/h. The landing is the reciprocal of the takeoff, as shown by the mirrored power curve.

Three different design options were created with various turbogenerator sizes. Once the turbogenerator was sized, the battery pack was sized accordingly to ensure the peak power of 560 kW could be supplied during takeoff. One interesting outcome of the battery sizing was that all three designs produced more battery capacity than required. In order to have a battery pack that could supply enough current (and power), cells needed to be added in parallel, which also increased the capacity. Different battery pack configurations were tried to eliminate the extra capacity and lower the battery mass, but the capacity is directly related to the current, so the extra capacity was unavoidable. To make use of this extra capacity, two different power strategies were proposed for each design. The first strategy has the turbine supply the same baseline power over the entire flight ($P_{Turbogen} = P_{Charge}$). The second strategy turns off the turbogenerator during cruise and supplies power only via the batteries ($P_{Turbogen} = P_{Charge}$). The results are presented below in Table 6.

Table 6: Results from the 3 design options chosen with the two different power strategies.

Option	Available Battery Capacity [kWh]	Turbogenerator On			Turbogenerator Off		
		DOH [%]	Battery Used [kWh]	Mass [kg]	DOH [%]	Time Off* [min]	Mass [kg]
350 kW	43.0	4.7	10.8	691	23.6	16	643
250 kW	64.4	9.8	17.2	724	46.0	22	676
150 kW	85.0	20.0	23.7	753	79.7	30	712

* Time that turbogenerator can be off until 90% of the battery capacity is used (max rated DOD) [21]

All three options have the same MTOW, which means that any deviation from the 700 kg target mass will result in an increase or decrease in payload. Turning the battery off during cruise can drastically increase the degree of hybridization (DOH) and reduce the power system mass due to the decrease in fuel mass. The same battery is used for both the turbine on and off strategies. The extra capacity, which was unavoidable, allows flexibility between the two scenarios. The three different battery packs are capable of supplying 213, 313 and 413 kW of power for the 350, 250 and 150 kW turbogenerators, respectively, which is more than enough to cover the 107 kW needed during cruise. For the turbogenerator on option, the turbogenerator is supplying more power than needed during cruise, which results in a worst-case scenario for DOH and power system mass. The power supply for the turbogenerator (P_{Charge}) will be altered once a design is chosen to optimize fuel consumption and develop a battery charging strategy. These results are presented in Figure 10 below.

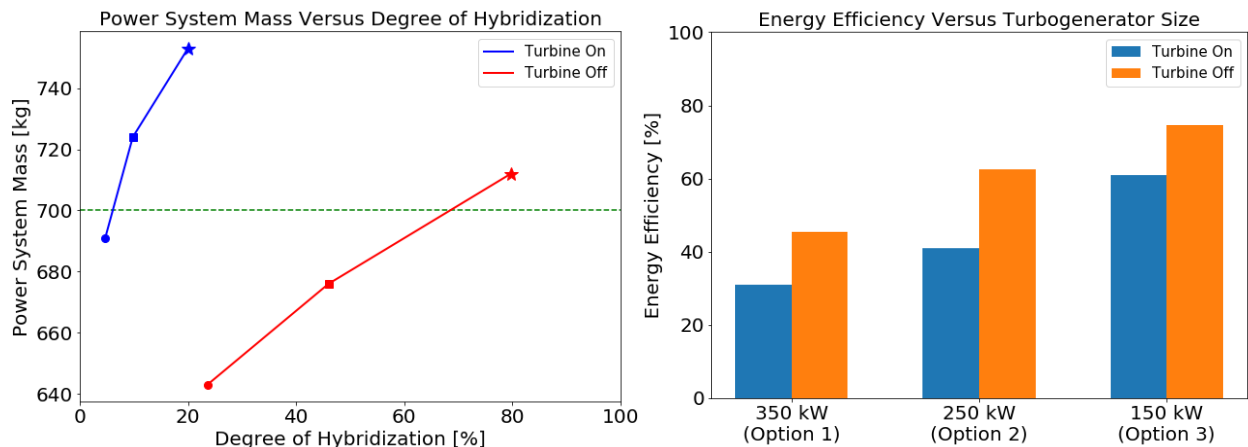


Figure 10: (Left) Power versus DOH. (Right) Energy efficiency for the three different options.

In the figure on the left, the circle represents option 1, the square option 2, the star option 3 and the green dotted line is the target mass of 700 kg. As expected, the DOH increases with mass, which highlights the difficulty in developing electric and hybrid aircrafts. By utilizing the extra battery capacity, the curve is shifted down and to the right, allowing lighter aircraft with higher DOH to be created. The red and blue lines create a bounding region for the designs. Once the turbogenerator power supply is optimized, each design is expected to operate somewhere between the blue and red data points. The figure on the right considers the energy efficiency of the aircraft, defined as the energy output at the propellers divided by the energy provided by the batteries and turbogenerator. This efficiency does not consider efficiencies related to electricity generation or fuel refinement; it treats the aircraft as an isolated system. As the

turbogenerator decreases in size, less excess power is being supplied which increases the efficiency. Turning off the turbogenerator further increases efficiency and ensures a larger portion of the energy put into the system is contributing directly to the output.

Equations 17 and 18 along with the battery capacity information in Table 6 were used to create the charging information for each design in Table 7.

Table 7: Charging information for the different design options and power strategies.

Option	$P_{MaxRate}$ [kW]	Turbogenerator On		Turbogenerator Off	
		Surplus Power Needed During Cruise [kW]	Downtime [min]	Charge During Cruise (while turbine on) [kWh]	Downtime [min]
350 kW	50.4	19.7	0	14.3	29.05
250 kW	75.6	31.3	0	13.9	34.97
150 kW	99.8	43.0	0	2.2	44.67

Based on the results of the simulation, the aircraft will be at its cruise speed for 33 minutes (0.55 hours). The larger the battery, the more power is needed for charging. $P_{MaxRate}$ represents the power required to charge each battery in 1 hour. If less power is supplied the battery will charge slower. All three options can be fully recharged during cruise, with the 150 kW option having just enough surplus power available to complete the charge. Turning off the turbogenerator significantly increases DOH, but this comes at the cost of increased charge time. Since the turbogenerator is not off for the entire cruise, some charging can be done in flight. The majority of charging will need to be done on the ground between flights. The downtime, shown in Table 7, only considers battery recharging and does not consider the time for refueling or passengers disembarking and boarding the aircraft. The DOD influences the capacity retention and cycle life of the battery [28]. Using more of the battery is good from an environmental and efficiency perspective, but it may lower the expected life of the aircraft, which could limit future economic returns.

Sensitivity Analysis

The simulation was used to conduct a sensitivity analysis on the mission parameters provided by the customer in Table 5. Each mission parameter was varied independently ($\pm 20\%$) and the total energy consumption for the flight was recorded to determine what input parameters have the most influence on total energy usage. The results are shown in Figure 11.

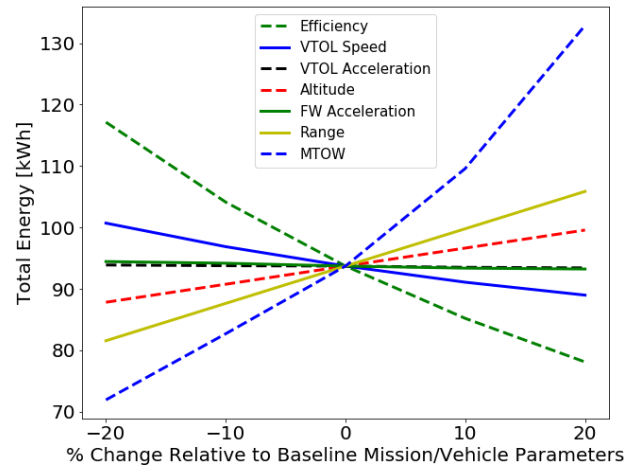


Figure 11: Sensitivity analysis of mission parameters on total energy consumption.

The magnitude of the slope indicates the sensitivity to a certain variable, the steeper slope means higher sensitivity, and the positive or negative slope indicates the direction of change. MTOW is the most sensitive, which is not a surprising result as mass is such a critical factor in all aviation applications. The analysis of MTOW required corresponding changes to the forward speed to ensure that the lift force was balancing the force of gravity, otherwise, a valid assessment could not be made. The efficiency, which accounts for the propellers and electric motors also had a significant impact on total energy. The range, altitude and VTOL speed have moderate impacts on the total energy. The VTOL and FW acceleration have very minimal impact on total energy, reflected by the flat slopes in Figure 11. The above figure is meant to aid in mission planning and the selection of components to maximize efficiency and minimize MTOW. Although not included in the figure, decreasing the FW speed results in the largest increase in total energy. This has such a significant impact because there are 8 VTOL that would require an additional 33 minutes of operation if there is not enough lift to balance gravity. Any increase in speed would require the VTOL propellers to pull the aircraft down, so increases in speed were not considered.

Environmental Considerations of Simulation

The environmental impact of each design is important to consider as it is one of the primary motivators for this type of technology, in addition to reducing commute times and ground transportation congestion. The total environmental impact per trip was evaluated by calculating kilograms of CO₂ expended by burning the required fuel amount and an assumed full battery charge from the grid. All energy values were converted to the equivalent kWh. Aviation fuel being burned produces around 3.16 kg of CO₂ per L burned [8]. This value was multiplied by the volume of aviation fuel consumed which has a density of 0.8 kg/L. The simulation provides the mass of fuel required for each design option and the amount of battery used, allowing the environmental impact to be considered.

The electrical grid in the province of Ontario was assumed to supply the electricity that would be used to charge the battery. In reality, the excess power from the turbogenerator could charge the batteries during flight, but for the sake of this analysis, all charging is assumed to be done on the ground, which provides a best-case scenario in terms of carbon emissions. Electricity in Ontario is generated in a variety of methods, predominantly hydro, natural gas and nuclear. This significantly lowers the emissions per kWh of electricity compared to charging with the turbogenerator. A comparison of the carbon emissions for each design option is shown in Table 8.

Table 8: CO₂ Emissions for Three Design Options

Option	Turbogenerator On During Cruise Kg CO ₂ [kg]	Relative Saving % to 350 kW baseline	Turbogenerator Off During Cruise CO ₂ [kg]	Relative Saving % to 350 kW baseline
350 kW	354.43	0	188.15	46.91
250 kW	262.32	25.98	92.58	64.70
150 kW	163.27	53.93	39.59	88.83

The choice to run the turbogenerator for the entire flight at baseline power significantly increases emissions and lowers the degree of hybridization due to both increasing the fuel burned and the higher associated carbon footprint of jet fuel. The emissions per kWh of aviation fuel are approximately 41 times higher than emissions per kWh from the Ontario electrical grid. Depending on where this aircraft is being used it is likely more environmentally friendly to utilize the grid for battery charging rather than the onboard turbogenerator.

9. Aircraft Stability Analysis

This section will cover the stability/moment coefficient analysis of the aircraft. This section is separated from the aerodynamic analysis section as this moment coefficient analysis required the locations and masses of each component. These variables were not known at the time of the initial aerodynamic analysis as the lift and drag coefficients were needed to find the component masses. The purpose of this analysis is to validate the aircraft's steady-state pitch stability, given the finalized locations of the components relative to the aircraft fuselage.

The objective of the stability analysis is to:

1. Prove that the moment coefficient plot has a negative slope for the final aircraft configuration
2. Ensure that the L/D is positive at the angle of attack where the moment coefficient is zero

These criteria ensure that the aircraft will be stable and capable of producing lift at the trim angle of attack (AOA). The trim AOA means the AOA at which the sum of moments about the CG (regarding pitch axis) is equal to zero. This analysis is limited to pitch and does not include yaw or roll as only pitch analysis was requested by the client, as this is more so a proof of concept. Optimizing the design for stability should involve modifying the aircraft airfoil's chord length, span, etc., in addition to point mass configuration, however, these modifications are outside the scope of this report. Consider the moment coefficient plot and the aircraft coordinate system presented below in Figure 12.

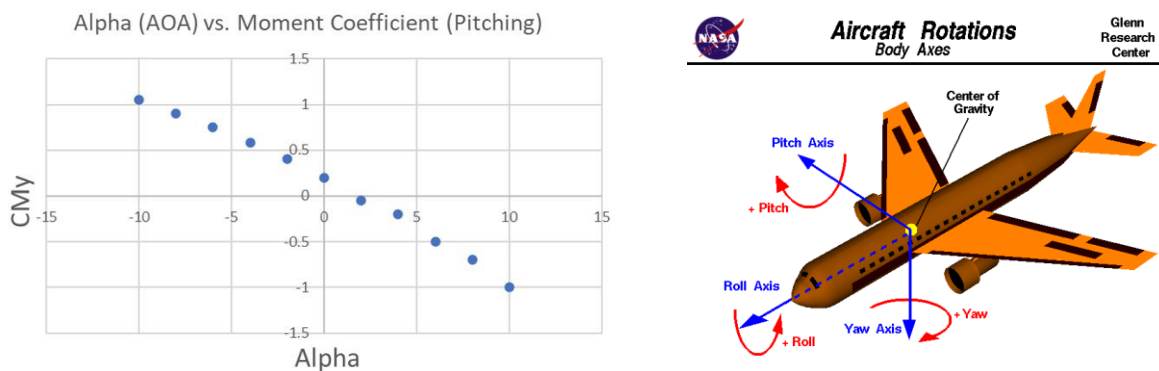


Figure 12: (Left) Example AOA vs. Moment Coefficient plot found using VSPAERO. (Right) Standard aircraft coordinate system.

The negative slope indicates that for an increase in alpha (AOA), the pitching moment becomes more negative. This is desirable since the pitching moment will counteract the change in AOA. Consider the aircraft coordinate system in Figure 12. a positive pitching moment will induce a nose-up movement, similarly, a negative pitching moment will induce a nose-down movement. Therefore, in a situation where a disturbance (e.g. wind gust) momentarily increases AOA (nose-up), the pitching moment will apply a nose-down moment, leveling the aircraft. If the slope of the AOA vs. moment coefficient curve is positive, a disturbance increasing AOA would incite a positive pitching moment on the aircraft. This would cause the aircraft to further increase its AOA and not reset to its initial position.

To compare the effect of component placement location on the stability of the aircraft, varying the battery location and recording its effect on stability was done using VSPAERO. Moving the heaviest, easiest to package component is most logical given that heavier objects will have a larger impact on stability. Further, moving components such as the propellers/motors is not as worthwhile given the limited available exterior design space. The battery was positioned rearward, mid, and toward the front of the

aircraft fuselage. The resulting slope of the moment coefficient curve, the trim state AOA, and the L/D value at this trim AOA are presented for a variety of component placement configurations in Table 9.

Table 9: Comparison of various aerodynamic stability parameters given varying battery positions within the aircraft

Configuration	Battery Location*	Turbogenerator Location	Slope of Moment Coefficient Curve [1/deg]	Trim State AOA [deg]	L/D Value at Trim AOA
1	Rear	Rear	-0.1	2	13
2	Mid	Rear	-0.14	1.5	11
3	Front	Rear	-0.2	0.5	7

** All batteries are located on the bottom of the fuselage*

As the battery moves forward, the trim state AOA decreases but the slope of the moment coefficient curve increases. In all cases modelled, the L/D is positive at trim AOA thus the aircraft could fly stably. As the batteries move forward, the L/D at the trim state AOA continually decreases. This may indicate a higher required top speed for the aircraft, given that the lift force is reducing. The slope of the moment coefficient curve indicates the magnitude of the pitching moment given an aircraft disturbance, where a larger slope (more negative, that is) indicates a larger moment. This may indicate greater stability, given that the disturbance is reacted by a larger counteracting moment. While a very low slope may not provide enough stability, and a very high slope may react too harshly to disturbances, it is not known what an ideal slope value is. For the final design, the batteries were placed in the middle-front of the fuselage.

The final stability concern is the draining of the fuel tank throughout the flight. In the VSPAERO model, the stability simulation was run with the full mass of the fuel tank, and with it removed. The location of the fuel tank, along with the final battery position, is pictured in Figure 13. The CG location in X (longitudinal axis) changed by 1.92%, the CG location in Z (vertical axis) changed by 8.93%, the slope of the moment coefficient curve changed by 8.96%, and the trim AOA changed from 1 to 0.6 degrees. These changes are not extremely significant, all being under 10% aside from the AOA change (which is relatively small compared to the full AOA range) and thus the placement of the fuel tank is deemed acceptable.

It has been proved that hybrid power system components can be placed in a way that produces stable flight. The magnitude of the moment coefficient slope and L/D value at the trim state will not be investigated further in this report, however, the values of these parameters could have a significant impact on component placement. Although stability “increases” when moving the batteries forward, determining a suitable corrective pitch moment which the pilot can manage must be determined. Further, with a varying L/D trim value per configuration, it must be considered how the component layout might alter required aircraft speed or potentially VTOL motor power during cruise. These considerations are recommended for future work.

10. Final Design

Power Strategy

After presenting the results discussed above to the client. The 250 kW turbogenerator option was selected. Although the 150 kW design had more environmental benefits, it did not meet the requirement for the power system mass. Even under the most optimal conditions it was 12 kg too heavy. The 150 kW option also provided less room for error in the calculation process. It is very likely that due to the oversimplification of the analysis process, the power is underestimated, which would make the 150 kW

option infeasible. The 250 kW option provides more of a safety factor in the design and would still be a suitable option if the actual power requirements were more than predicted. Based on the level of analysis done, the 250 kW option is the most suitable choice, although much more detailed analysis should be completed to confirm these findings. To allow the client flexibility in their usage of the UAM vehicle, three different power strategies are being suggested for the 250 kW design. The first option runs the turbine continuously during cruise. Enough surplus power is provided via the turbogenerator to fully charge the battery during the 33 minute cruise. The second option does not recharge during cruise, rather, it decreases the power output, so the turbogenerator supplies just enough power for the electric motors. The third option uses the extra battery capacity to completely turn off the turbogenerator during cruise. The expected results from the three options are shown below in Table 10.

Table 10: Results for the 3 different power strategies presented for the 250 kW turbogenerator design.

Power Strategy	DOH [%]	Power System Mass [kg]	Payload [kg]	Downtime [min]	P_{cruise} [kW]	Fuel Used [kg]
Option 1	15.1	693	507	0	139	50.8
Option 2	17.8	683	517	13.65 - 40.95	107	41.5
Option 3	51.1	670	530	34.97	183*	28.3

* The turbine is off for 22 min, leaving 11 min to charge ($P_{MaxRate}$ is supplied)

The results in the table above highlight one of the tradeoffs in the design. In order to have a short downtime between flights, more fossil fuels need to be used. The power strategies here have been modified slightly compared to the results section. The turbogenerator output has been adjusted during cruise to supply only the power needed, excess power is no longer being supplied. The turbogenerator efficiency will decrease at lower power outputs, which has not been considered in this analysis due to the time constraints of the project [12]. It is recommended that this aspect of the design be investigated in the future to better assess the accuracy of the results in Table 10. The same battery is used for all three power strategies, meaning that each of the three options can be implemented on the same aircraft, allowing the client flexibility in the scheduling and usage of the aircraft. The only changes required between options is the amount of fuel needed and the control of the turbogenerator. If there is high demand, the less environmentally friendly option 1 can be used. This option may also be used if one of the destinations has only refueling infrastructure and not charging infrastructure. The second option may be used when a slightly higher degree of hybridization is preferred. This option requires 14 minutes to recharge after a single trip or can complete 3 trips on a single charge, which will take 41 minutes. The third option can be used when scheduling and infrastructure allow for charging between flights. One downside of option 3 is that the high DOD may shorten the cycle life of the batteries. An additional benefit of the design is that the extra battery capacity allows the range of the vehicle to be extended if desired and provides additional flying time in the event of emergencies. The battery is capable of powering the aircraft at its cruise speed of 264 km/h for 22 minutes, while still having the enough capacity for takeoff and landing, which corresponds to an additional 96 km of range.

Bill of Materials

The final components selected by the team are detailed in Table 11.

Table 11: Bill of materials for the final design.

Component	Model / Manufacturer	Mass	Quantity
Turbogenerator	Honeywell	88.5 kg	1
Motors	Emrax 268 (High Voltage) [17]	20.5 kg	10
Propellers	MT-Propeller [24]	4.15 kg	10
Lithium-Ion Cell	NMC811-20 [21]	1.8 kg (per cell)	150

Note that the 88.5 kg turbogenerator mass is based on assumptions as a mass was not provided by the supplier. The same components are capable of executing all three power strategies presented above. The component placement in the fuselage is shown in Figure 13.

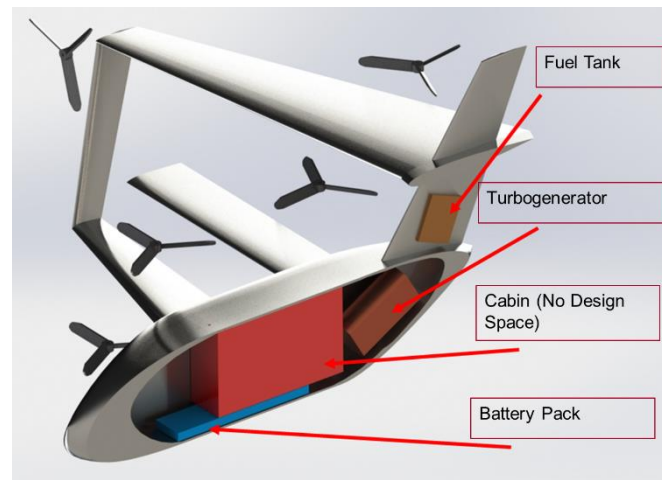


Figure 13: Final power system component layout and propeller placement.

Turbogenerator

A 250 kW Honeywell turbogenerator is being recommended. Before implementing the design, the supplier should be contacted to get accurate specifications for the turbogenerator and to discuss the power strategy to develop a design that will operate at the highest possible efficiency. As discussed in the Turbogenerator Sizing section, the power density was approximated using a 330 kW turbine and a 250 kW generator and scaling to fit the supplied power. Since the final design utilizes a power output in the same range, it is assumed for the purposes of this preliminary design that the assumptions made regarding the turbogenerator are valid.

Batteries

Based on the 250 kW turbogenerator, the batteries must be capable of supplying 310 kW of power. Using the high voltage electric motor produces the lightest battery pack, with a total mass of 297 kg, containing 150 total cells (individual batteries). This battery pack configuration requires 25 cells in series and 6 cells in parallel. Note that this mass includes 10% extra mass for cooling systems, which should be investigated in more detail. The low voltage model could also be used to produce a similar battery pack that is 4 kg heavier and uses an extra 2 cells (8 in series, 19 in parallel). The total volume of the battery pack is 0.1249668 m^3 . The battery pack in Figure 13 is two cells high and has a footprint of 1.0773 m^2 , which allows it to be easily placed within the fuselage. The battery pack shape is highly customizable and future research may be needed to determine the safest/best configuration. Depending on the cooling system, a larger surface area may be required which would increase the battery footprint.

Electric Motors

To supply enough power for VTOL, the motors selected for the final design are the EMRAX 268 High Voltage liquid-cooled motors. Each motor is capable of 73 kW of continuous power, 213 Nm of continuous torque and the high voltage package has the highest torque per motor current (Nm/Arms) of the configurations [17], reducing the need for as many in-parallel battery cells. The liquid cooling system also has the highest ingress protection of IP65, meaning the motors can be placed on the outside of the fuselage and be safely run in wet or dusty weather conditions. The rated efficiency is between 93% and 98% so the average of 95.5% was implemented in the simulation [17].

Propellers

8 VTOL and 2 forward 1.5 m diameter MT-natural composite propellers are recommended for the design. These propellers are rated to motor power up to 298.28 kW, which is over 4 times the peak power any individual propeller will be subjected to. Further, at a density of 0.7 g/cm^3 , these propellers are some of the lightest in the market, allowing a weight of approximately 50% of current metal propellers [24]. A propeller efficiency of 80% was assumed based on the approximate airspeed of 250 km/h [29]. The exact efficiencies and their relationship with RPM and airspeed should be requested from the supplier.

Environmental Impact

Based on the customer selection of the 250 kW baseline power configuration, CO₂ emissions can be calculated for each of the three power strategies detailed below in Table 12.

Table 12: CO₂ Emissions for three 250 kW Power Strategies.

Option	Fuel Consumed [L]	Emissions from Fuel [kg CO ₂]	Electricity for Charging [kWh]	Emission from Grid Charging [kg CO ₂]	Total Emissions [kg CO ₂]	Relative Percentage Savings
1	10.07	31.82	0	0	31.82	0%
2	8.24	26.04	17.2	1.32	27.36	14%
3	5.60	17.71	44.06	3.39	21.1	33.68%

This table shows the advantages of turning the turbogenerator off during cruise. It also highlights that option two is more environmentally friendly option as the emissions associated with recharging the batteries using the grid are low.

Vehicle Comparison

A comparison of environmental impact was then performed between the UAM hybrid vehicle design and a conventional car and helicopter in terms of CO₂ emissions along with total trip time. This was done to mimic a single commute to compare the three modes of transportation. The car was assumed to travel at a constant speed of 80 km/h and the helicopter was assumed to travel at a speed of 204 km/h [30]. These velocities were derived using 80% of each vehicle's maximum speeds during travel. This percentage was selected to compensate for stop-and-go traffic and takeoff and landing for the car and helicopter, respectively. The results of this comparison are summarized in Table 13, where the CO₂ savings are expressed in terms of the helicopter CO₂ emissions and trip time was calculated for a 150 km trip.

Table 13: Comparison of emissions and trip times of similar vehicles the UAM aircraft.

Vehicle	CO2 Emissions (kg)	CO2 Savings	Trip Time (min)
Car	18.57 [31]	76%	112.5
UAM Vehicle	31.82	58%	38
Helicopter	76.65 [32]	0% (Ref)	44

Based on the vehicle trip comparison, it can be concluded that the UAM vehicle was the quickest form of travel. Additionally, the UAM is a significant fuel saver compared to the helicopter for the same trip length. Although the car shows greater emissions savings, it should be noted that the car will produce significantly more emissions during stop-and-go traffic, especially in highly populated cities. It can be concluded that implementing the UAM vehicle into urban cities can greatly reduce commute times and has the potential to reduce emissions if there is heavy traffic, although this needs to be further researched.

Cost Analysis

The operational cost of the aircraft is significant and not to be understated. In addition to both fuel and electrical consumption, the aircraft must receive regular maintenance for the various power system components. Most notably, the Rolls Royce M250 gas turboshaft engine or equivalent Honeywell turbogenerator unit must receive maintenance and inspections at regular intervals.

Maintenance intervals are usually described in run-time hours or restart cycles, whichever is lower [33]. The RR M250 compressor and turbine stages for example have a maximum run time of 3500 hours and will require maintenance. A Hot Section Inspection (HSI) is required halfway between maintenance intervals, putting the required inspection at a conservative 1750 hour run time [34]. The cost for an HSI and compressor wheel replacement is approximately \$55,000 [35]. A conservative cost per operating hour is ~\$32/hr for maintenance alone or ~\$20.20/trip (0.631 hr/trip).

Further costs are incurred by charging and discharging the lithium-ion batteries. Batteries are rated for a finite number of charge-discharge cycles after which capacity and performance is reduced. The Greypow batteries are rated for 90% capacity retention after 600 cycles [21]. This value will be used to provide a conservative estimate of when the batteries need to be replaced. Battery replacement costs are estimated based on the total capacity, 64.4 kWh and the market average for lithium-ion cells of \$175.26 CAD per kWh [36]. This leads to an approximate cost of \$11,286.74. Assuming each trip consists of one charge-discharge cycle the batteries can complete 600 trips, for a cost of \$18.80/trip. Recall that option 2 is capable of completing 3 trips on a single charge, decreasing the cost to \$6.27/trip.

Option one provides a solely fuel-based strategy, with 96.7 kWh used and 2.45 Gallons of fuel. The cost of jet fuel as of October 2021 is \$2.86 CAD per US gallon [37]. These costs are derived from bulk pricing and would likely be higher for any given carrier that is paying for fuel to be supplied to its fleet. Electrical costs are derived from the battery capacity that must be filled by charging from the grid. The current electrical cost for Ontario is \$0.13/kWh [38]. The associated operational costs are shown in Table 14.

Table 14: Operation cost for three design options.

Option	Fuel cost per Trip [CAD]	Electrical Cost per Trip [CAD]	Operation Cost per trip [CAD]
1	6.63	0	45.63
2	5.41	1.41	33.29 – 45.82
3	3.46	3.60	46.06

Many powerplant manufacturers such as Pratt & Whitney, Rolls Royce, Turbomecca, and others offer power by the hour (PBH) support services [39]. These PBH or support by the hour (SBH) programs manage risk and cost for operators. These services include parts, maintenance, and loaned engines if required due to service delays or unexpected problems. These services are not accounted for in the above costing. Furthermore, staffing costs related to piloting and ground support crews are not included.

The majority of the power system cost is made up of the turbogenerator (\$323,400) [40], batteries (\$11,286.74) [36], motors (\$10,076.56 each) [41] and propellers (\$1034.00 each) [42]. The Honeywell 250 kW turbogenerator is a relatively new unit, and its approximate cost is not known. The Rolls Royce M250 Turboshaft price at the high end of its range was substituted. The overall cost for the power system consisting of batteries, turbogenerator, motors, and propellers is \$445,792.34 CAD. This does not include cooling and motor controllers, therefore, the value provided above is an underestimate.

Final Recommendation

Although three different options are being presented, option 2 is suggested as the best power strategy to use at this time. This decision was made after the client expressed their desire for the turbogenerator to be on for the entire flight. Option 1 and 2 both have the turbogenerator on for the entire flight, but option two has fewer carbon emissions, due to charging using the grid rather than the turbogenerator and lower operating costs. The downtime of 14 minutes between flights is relatively short and would likely not interfere with scheduling as time would be needed for passengers to get on and off of the aircraft. Option 3 provides more environmental benefits but uses a relatively unconventional approach of turning the turbogenerator off during flight. Due to limited research into the logistics of this option, it is not being recommended at this time, but because of the significant potential increase in DOH it should be considered further in the future. Some areas to consider before implementing option 3 would be:

- Repeatability of starting the turbogenerator electronically using the batteries, failure to start would be very dangerous.
- Investigate the resulting increase in maintenance on the turbogenerator from increased on/off cycles.
- Determine if there are any regulatory constraints that would prevent this type of operation.

11. Future Work

The research presented in this document details a feasible preliminary design for a UAM vehicle power system however, there is much more that can be done to improve and validate the design. Due to the limited time frame for this project and limited component information from suppliers, many assumptions and simplifications were made that should be further explored.

The simulation was a major part of the design process, but there is significant room for improvement in the accuracy of the results it can achieve. The most obvious areas of improvement for the simulation are listed below:

- Create a more realistic flight profile, with a VTOL, climb, and cruise stage
- Include non-linear accelerations and consider a non-symmetrical profile to account for air braking
- Get detailed efficiency specifications for the turbogenerator and propellers
- Include an aerodynamic analysis of fuselage with propellers and booms

The battery is a critical component, and the battery technology is the limiting factor in the design. Battery technology is rapidly advancing, and better-suited batteries may reach the market in the near future. Due to the limited time frame and countless possible battery configurations, a significant area of future research is the continued remodeling of battery pack sizing and configuration. Due to the time constraints of the project very little research was done on proper battery management. This is a vast topic and will likely influence the charging strategy, battery climate control and battery pack configuration. Additional research may also be done to figure out if it's possible to reduce the excess battery capacity while still supplying enough power.

The manufacturers of the components used in the design should be contacted to confirm the dimensions and costs of each part. As the highest cost and specific component, the turbogenerator is the most affected by any discrepancies in the mentioned dimensions. This step is necessary to justify the feasibility of the power system design.

One area that was not addressed was the cabin noise produced from this power system design. The turbogenerator will produce significant noise and vibration, which will need to be controlled. For the current design to be implemented into a working prototype, research into noise control and vibration dampening needs to be done.

12. Conclusion

The finished design can be evaluated against the targets identified in the bottom row of the QFD seen in Appendix A. A 50% degree of hybridization was not realized, and the cabin noise was not analyzed however, this is something that should be considered moving forward. From a qualitative perspective, the noise was reduced by placing the turbogenerator as far from the cabin as possible to eliminate noise and although this option is not being suggested, turning off the turbogenerator during cruise would create a much quieter cabin. The 50% DOH is possible with option 3 presented above, but due to limited research into the logistics of this strategy and the client requests, it is not being suggested. Currently, the DOH is 17.8% but there is potential to reach the 50% threshold. All other design targets were met, including range, cruise altitude, power system mass, fuel reserve, total cost, and stable flight.

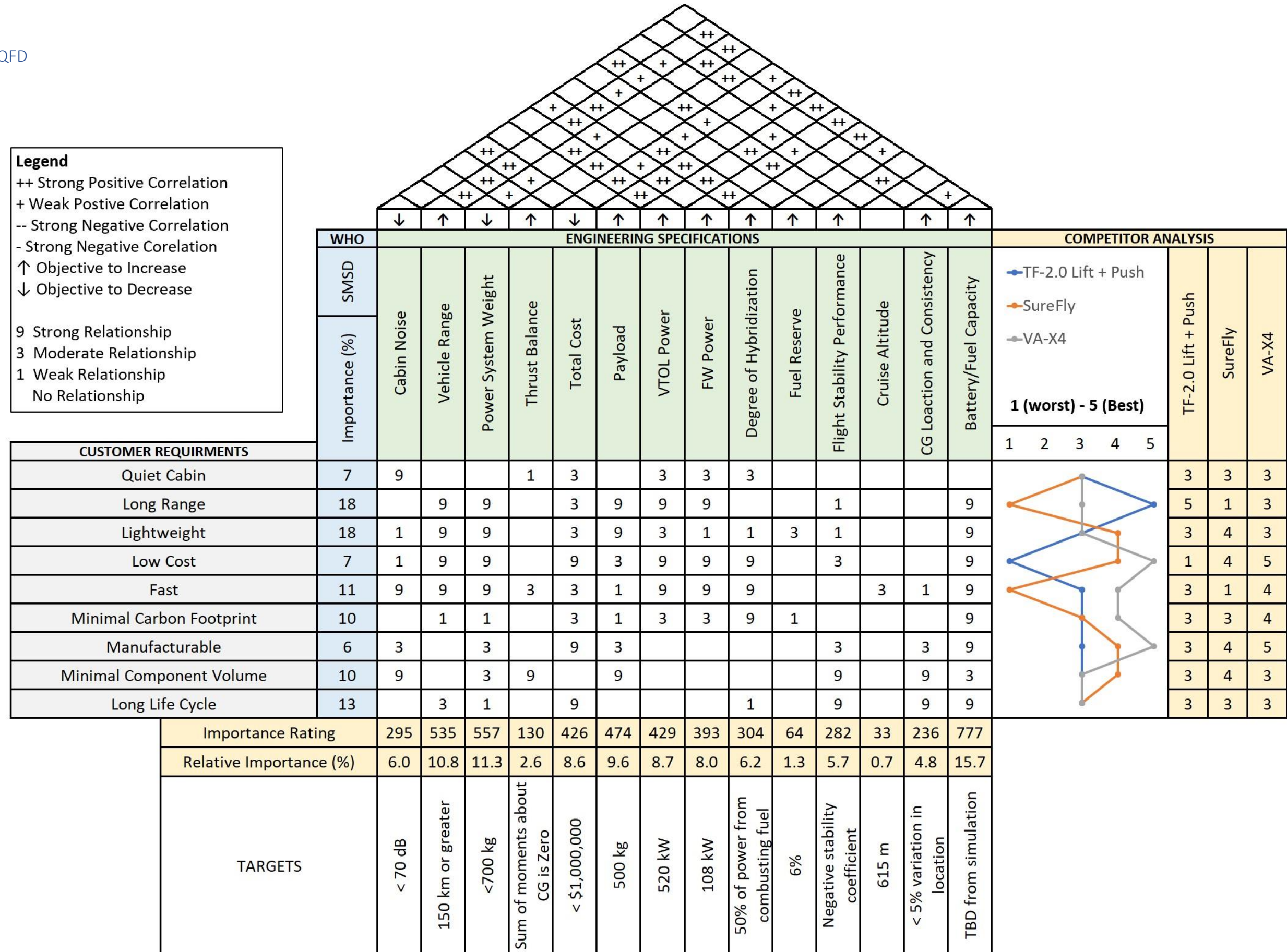
The UAM vehicle is feasible with today's technology and could be implemented effectively. The market viability of the UAM is directly dependent on battery energy density and mass. Future improvements in battery technology will make hybrid UAM vehicles a more competitive alternative to current transport infrastructure and traditional propeller or rotary-wing aircraft for inter-city travel. Current technology limits the degree of hybridization of a hybrid UAM but does not prevent its implementation. Higher battery capacity increases the degree of hybridization but detracts from the feasibility of a UAM with current technology due to increased downtime for charging and increased mass. At the time of writing, a traditional fossil fuel-powered aircraft is a financially superior and more flexible form of transport.

References

- [1] Vertical Flight Society, "Terrafugia TF-2.0 Lift + Push," 2021. [Online]. Available: <https://evtol.news/terrafugia-tf-2-lift-push/>.
- [2] Vertical Flight Society, "Moog SureFly," 2021. [Online]. Available: <https://evtol.news/workhorse/>.
- [3] Tom Phillips, "Electric air taxis to make their debut in Brazil's most congested city," 21 September 2021. [Online]. Available: <https://www.theguardian.com/world/2021/sep/21/electric-air-taxis-sao-paulo-brazil>.
- [4] Jon Hemmerdinger, "Gol to acquire 250 of Vertical Aerospace's in-development VA-X4 from lessor Avolon," 21 September 2021. [Online]. Available: <https://www.flightglobal.com/aerospace/gol-to-acquire-250-of-vertical-aerospaces-in-development-va-x4-from-lessor-avolon/145566.article>.
- [5] Clean Energy Institute University of Washington, "Lithium-Ion Batteries," 2021. [Online]. Available: <https://www.cei.washington.edu/education/science-of-solar/battery-technology/>.
- [6] Brian Garrett-Glaser, "The Batteries Behind the Electric Aircraft Revolution," 8 September 2020. [Online]. Available: <https://www.aviationtoday.com/2020/09/08/batteries-behind-electric-aircraft-revolution/>.
- [7] Battery University, "BU-808: How to Prolong Lithium-based Batteries," 2019. [Online]. Available: <https://batteryuniversity.com/article/bu-808-how-to-prolong-lithium-based-batteries>.
- [8] J. Schenderlein and T. Clayton, "Comparison of Helicopter Turboshaft Engines," [Online]. Available: https://www.colorado.edu/faculty/kantha/sites/default/files/attached-files/16496-116619_-_tyler_clayton_-_dec_17_2015_110_pm_-_clayton_schenderlein_comparisonofhelicopterengines.pdf. [Accessed September 2021].
- [9] D. B. Harrington, "Turbine Generators," Science Direct , 2003.
- [10] Honeywell International Inc, "60kVA Generator," 2021. [Online]. Available: <https://aerospace.honeywell.com/us/en/learn/products/electric-power/60kva-generator>.
- [11] "Pratt & Whitney - Helicopter Engines," [Online]. Available: <https://www.pwc.ca/en/products-and-services/products/helicopter-engines>.
- [12] T. Donato, A. Carla and G. Avanzini, "Fuel Consumption of Rotorcrafts and Potentiality for Hybrid Electric Power Systems," *Energy Conversion and Management* , no. 164, pp. 429-442, 2018.
- [13] M. B. & K. Hall-Geisler, "How Electric Motors Work," howstuffworks, 5 October 2021. [Online]. Available: <https://electronics.howstuffworks.com/motor.htm>. [Accessed October 2021].
- [14] A. Lavaa, "What is Axial Flux Motor and It's Working Principle?," Linqip Technews, 24 August 2021. [Online]. Available: <https://www.linqip.com/blog/what-is-axial-flux-motor/>. [Accessed October 2021].
- [15] D. P. Raymer, Aircraft Design: A Conceptual Approach, Washington, D.C.: American Institute of Aeronautics and Astronautics, Inc..
- [16] "Introduction to Propeller of Vertical Take-off and Landing Fixed Wing UAV," JOUAV, 25 March 2021. [Online]. Available: <https://www.jouav.com/news/introduction-to-propeller-of-vertical-take-off-and-landing-fixed-wing-uav.html>. [Accessed 21 October 2021].
- [17] EMRAX, "https://emrax.com/wp-content/uploads/2020/03/emrax_268_technical_data_table_graphs_5.4.pdf".
- [18] AVID Technology, "<https://avidtp.com/product/evo-motors/>".
- [19] C. Nuamah, "A Simple Comparison of Six Lithium-ion Battery Types," 23 August 2021. [Online]. Available: <https://owlcation.com/stem/Comparing-6-Lithium-ion-Battery-Types>.
- [20] Battery University, "Types of Lithium-ion," 2021. [Online]. Available: <https://batteryuniversity.com/article/bu-205-types-of-lithium-ion>.
- [21] Grepow Rechargeable Battery, "New Technology - NMC 811 Battery," 2021. [Online]. Available: <https://www.grepow.com/page/nmc-811-battery.html>.
- [22] Honeywell International Inc, "250kW Generator," 2021. [Online]. Available: <https://aerospace.honeywell.com/us/en/learn/products/electric-power/250kw-generator>.
- [23] YASA Limited, "<https://www.yasa.com/wp-content/uploads/2021/05/YASA-P400RDatasheet-Rev-14.pdf>," 2019.

- [24] MT-Propeller, "Fixed Pitch MT-Propellers," January 2019. [Online]. Available: https://www.mt-propeller.com/en/entw/pro_fixed.htm. [Accessed 10 November 2021].
- [25] "Speed of Sound," NASA, 13 May 2021. [Online]. Available: <https://www.grc.nasa.gov/www/k-12/airplane/sound.html>.
- [26] "Disk loading," Wikipedia, [Online]. Available: https://en.wikipedia.org/wiki/Disk_loading. [Accessed 25 October 2021].
- [27] Honeywell Aerospace, "T53 Turboshaft Engine," 2019. [Online]. Available: <https://aerospace.honeywell.com/content/dam/aerobt/en/documents/learn/products/engines/brochures/N61-1733-000-000-T53-v6-bro.pdf>.
- [28] World Electric Vehicle Journal Vol.8, "Degradation mechanism detection for NMC batteries," 19 June 2016. [Online]. Available: <file:///C:/Users/Luke%20Ulsifer/Downloads/wevj-08-00350.pdf>.
- [29] Czech Technical University Aerospace Engineering, "Increase of the Propellor Efficiency by Variable RPM," 2017. [Online]. Available: <https://www.dglr.de/publikationen/2017/450176.pdf>.
- [30] K. Gatto, "Eurocopter X3: The world's fastest coptor," Phys.org, 20 May 2011. [Online]. Available: <https://phys.org/news/2011-05-eurocopter-x3-world-fastest-copter.html#:~:text=An%20average%20helicopter%20can%20reach,in%20stable%20and%20level%20flight..>
- [31] European Environment Agency , "CO2 Performance of new passengers cars in Europe," European Environment Agency , 18 November 2021. [Online]. Available: https://www.eea.europa.eu/ims/co2-performance-of-new-passenger?fbclid=IwAR3xR2D5UtvNxEbvDLFe5-LjDrMEJuU5Ey_-_axdUfJM58thq_TnxAX9fjk.
- [32] P. Paoster, "What About Helicopter Emissions," Environmental News Network , 1 October 2007. [Online]. Available: https://www.enn.com/articles/23533-what-about-helicopter-emissions?fbclid=IwAR08_pwq5_WBwvWtrtUIbeXUeBn8A6yLSF-07UMHEiEwNfHatIE86wleCK8.
- [33] Rolls Royce, "250–C20 SERIES OPERATION AND MAINTENANCE," [Online]. Available: https://pscorp.ph/wp-content/uploads/2019/06/250-C20-Operation-Maintenance-Manual_6th_ED_Rev.16.pdf. [Accessed November 2021].
- [34] Pratt and Whitney Canada, "Why Your Engine Needs a Hot Section Inspection," 2019. [Online]. Available: <https://www.pwc.ca/en/airtime-blog/articles/technical-tips/why-your-engine-needs-a-hot-section-inspection>. [Accessed 25 November 2021].
- [35] "C20B Overhaul Costs," 2015. [Online]. Available: <https://www.pprune.org/rotorheads/565460-c20b-overhaul-costs.html>. [Accessed 23 November 2021].
- [36] V. Henze, "Battery Pack Prices Cited Below \$100/kWh for the First Time in 2020, While Market Average Sits at \$137/kWh," 16 December 2020. [Online]. Available: <https://about.bnef.com/blog/battery-pack-prices-cited-below-100-kwh-for-the-first-time-in-2020-while-market-average-sits-at-137-kwh/>. [Accessed 25 November 2021].
- [37] Miguel Barrientos , "Jet Fuel Monthly Price - Canadian Dollars per Gallon," Index Mundi , 2021. [Online]. Available: <https://www.indexmundi.com/commodities/?commodity=jet-fuel&months=12¤cy=cad>. [Accessed 25 November 2021].
- [38] R. Urban, "Electricity Prices in Canada 2021," 11 March 2021. [Online]. Available: <https://www.energyhub.org/electricity-prices/>. [Accessed 26 November 2021].
- [39] A. Drweiga, "Maintaining Engine Maintainace Expenses," 1 November 2014. [Online]. Available: <https://www.rotorandwing.com/2014/11/01/maintaining-engine-maintenance-expenses/>. [Accessed 21 November 2021].
- [40] J. Kasper and O. Balle, "Rolls-Royce M250 Turboshaft," Forcast International , 2020. [Online]. Available: <http://www.fi-powerweb.com/Engine/Rolls-Royce-M250.html>. [Accessed Decmeber 2021].
- [41] Emrax, "Emrax Configurator," Emrax, 2020. [Online]. Available: <https://emrax.com/get-a-quote/?configaction=shop>. [Accessed December 2021].
- [42] Aircraft Spruce , "WARP DRIVE ADVANCE COMPOSITE PROPELLERS," 2021. [Online]. Available: <https://www.aircraftspruce.ca/catalog/appages/warpdrive.php>. [Accessed Decemeber 2021].

Appendix A – QFD



Appendix B – Weighted Evaluation Matrices

Table 15: Weighted evaluation matrix for the 3 different battery options.

			BATTERIES					
			NMC		NCA		LTO	
Criteria	Weighting	Error	Rank	Score	Rank	Score	Rank	Score
Cost	9.4	1.1	3	28.2	2	18.8	1	9.4
Specific Energy	38.2	1.5	2	76.4	3	114.6	1	38.2
Specific Power	17.8	1.5	2	35.6	1	17.8	3	53.4
Safety	13.8	2.8	2	27.6	1	13.8	3	41.4
Performance	8.6	2.2	2	17.2	1	8.6	3	25.8
Cycle Life	12.2	2.3	2	24.4	1	12.2	3	36.6
Total	100			209		186		205
±				10		7		14

Table 17: Weighted evaluation matrix for the 3 different VTOL propellor configurations.

			VTOL PROPELLERS					
			Wing Embedded		Boom Mounted on Wings		Boom Mounted Wings + Fuselage	
Criteria	Weighting	Error	Rank	Score	Rank	Score	Rank	Score
Mass	16.8	4.3	3.0	50.4	2.0	33.6	2.0	33.6
Stability and Balance	25.0	1.4	2.0	50.0	2.0	50.0	3.0	75.0
Ability to Fit Multiple Propellers	29.0	2.2	1.0	29.0	2.0	58.0	3.0	87.0
Design Volume Required	10.4	3.6	3.0	31.2	2.0	20.8	1.0	10.4
Effect on Control Surface Effectiveness	18.8	9.3	1.0	18.8	2.0	37.6	2.0	37.6
Total	100			179		200		244
±				20		22		22

Table 16: Weighted evaluation matrix for the 3 different electric motors.

			ELECTRIC MOTOR					
			YASA P400 R		EVO AF140		EMRAX 268	
Criteria	Weighting	Error	Rank	Score	Rank	Score	Rank	Score
Size/profile	22.6	1.8	2	45.2	1	22.6	3	67.8
Mass	25.8	5.8	2	51.6	1	25.8	3	77.4
Continuous Power	27	2.7	1	27	3	81	2	54
Peak Power	11.4	1.7	1	11.4	3	34.2	2	22.8
Maximum RPM	13.2	4.1	3	39.6	2	26.4	1	13.2
Total	100			175		190		235
±				18		14		20